Riv. Mat. Univ. Parma, Vol. **2** (2011), 147-187

A. AIMI, M. DILIGENTI and C. GUARDASONI

Numerical integration schemes for applications of energetic Galerkin BEM to wave propagation problems

Abstract. Here we consider wave propagation problems with vanishing initial and mixed boundary condition reformulated as space-time boundary integral equations. The energetic Galerkin boundary element method used in the discretization phase, after a double analytic integration in time variables, has to deal with weakly singular, singular and hypersingular double integrals in space variables. Efficient numerical quadrature schemes for evaluation of these integrals are here proposed. Several numerical results are presented and discussed.

Keywords. Energetic Galerkin BEM (hyper)singular integral, quadrature rule.

Mathematics Subject Classification (2000): 65D30, 65N38.

Contents

Received: July 19, 2010; accepted: October 19, 2010.

1 - Introduction

Linear time-dependent two and three-dimensional problems are ideally suited to successful applications of boundary integral equation (BIE) approaches and to their discretizations into boundary element methods (BEMs). Frequently claimed advantages over domain approaches are the dimensionality reduction, the easy implicit enforcement of radiation conditions at infinity and the high accuracy achievable. Excellent survey on the available literature on BIE and BEM in time-dependent problems can be found in [**11, 12**]. The transformation of the problem to a boundary integral equation follows the same well-known method for elliptic boundary value problems. Most earlier contributions concerned direct formulations of BEM in the frequency domain, often using the Laplace transform and addressing wave propagations problems. The pioneering work of Cruse and Rizzo [**13**] and the results in [**2, 8, 15, 16, 18, 26, 28**] are among the standard references in the field.

Time-domain direct BIE formulations were developed more recently, primarily stimulated by soil-structure interaction problems. In this case, the representation formula in terms of single layer and double layer potentials uses the fundamental solution of the hyperbolic partial differential equation and jump relations, giving rise to retarded boundary integral equations [**9, 10**]. These approaches lead in the discretization phase to systems of linear equations with nonsymmetric coefficient matrices, to be solved for each time step. Symmetric formulations were proposed in [**26, 34**].

Usual numerical discretization procedures include collocation techniques and Laplace-Fourier methods coupled with Galerkin BEM in space. The application of Galerkin BEM in both space and time has been implemented by several authors but in this direction only the weak formulation due to Ha Duong [**20**] and Ha Duong et al. [**21**] furnishes genuine convergence results. The only drawback of the method is that it has stability constants growing exponentially in time, as stated in [**12**].

The convolution quadrature method for the time discretization has been developed in [**23, 24, 25**]. This method has the fundamental property of avoiding using the explicit expression of the kernel which is instead replaced by that of its Laplace transform. These rules do not have any degree of exctness, however the convergence properties are guaranteed under certain assumptions on the above Laplace transform and on the density function.

Recently, we have considered 2D Dirichlet or Neumann problems for a temporally homogeneous (normalized) scalar wave equation outside an obstacle Γ in the time interval $[0, T]$, reformulated as a boundary integral equation with retarded potential.

Special attention was devoted to a natural energy identity related to the differential problem, that leads to a space-time weak formulation for the BIEs, having, under suitable constraint, precise continuity and coerciveness properties (see [**4, 5**]).

The related energetic Galerkin BEM formulation is discretized in time and space, and it is shown that the time integrations can be performed analytically. A time marching scheme is set up to numerically solve the resulting BIE. The spatial singularity of the resulting kernels are investigated and shown to be exactly those found in the static case. As a consequence of this, the treatment of the singular and hypersingular double integrals (see [**19**]) in space variables can be similar to that devised for this simpler case. Krishnasamy el al. [**22**] have introduced a hypersingular formulation for time-harmonic three-dimensional elastic wave scattering by cracks and discussed different alternatives for the computation of the hypersingular integrals. Sládek and Sládek [**35**] solved the same problem by Laplace transform method, but they also remove the hypersingular integrals by partial integrations. Recent overviews, properties and applications of finite-part integrals have been presented by Monegato [**33**].

In this paper, we consider all integrals whose evaluation is required by Galerkin BEM based on piecewise polynomial approximants of arbitrary local degrees. To compute these integrals we propose efficient quadrature schemes. In the last section various numerical results will be presented and discussed.

2 - Model problem and its energetic boundary integral weak formulation

We consider a mixed boundary value problem for the wave equation with homogeneous initial conditions, in a bounded, simply connected, domain $\Omega \subset \mathbb{R}^2$, with a boundary Γ referred to a Cartesian orthogonal coordinate system $\mathbf{x} = (x_1, x_2)$ and partitioned into two non intersecting subsets Γ_u and Γ_p ($\Gamma_u \cap \Gamma_p = \emptyset$) such that $\overline{\Gamma} = \overline{\Gamma}_u \cup \overline{\Gamma}_p$. Without loss of generality we will consider a dimensionless problem which can be obtained after an appropriate scaling of the units

$$u_{tt} - \triangle u = 0, \qquad \mathbf{x} \in \Omega, \;\; t \in (0, T) \tag{1}$$

$$u(\mathbf{x}, 0) = u_t(\mathbf{x}, 0) = 0, \qquad \mathbf{x} \in \Omega \tag{2}$$

$$u(\mathbf{x}, t) = \bar{u}(\mathbf{x}, t), \qquad (\mathbf{x}, t) \in \Sigma_T^u := \Gamma_u \times [0, T] \tag{3}$$

$$p(\mathbf{x}, t) := \frac{\partial u}{\partial \mathbf{n}}(\mathbf{x}, t) = \bar{p}(\mathbf{x}, t), \qquad (\mathbf{x}, t) \in \Sigma_T^p := \Gamma_p \times [0, T] \tag{4}$$

where $\mathbf{n}$ is the unit outward normal vector of Γ, $\bar{u}$ and $\bar{p}$ are given boundary data of Dirichlet and Neumann type, respectively.

Let us consider the boundary integral representation of the solution of (1)-(4) for $\mathbf{x} \in \Omega$ and $t \in (0, T)$ (see [27])

$$u(\mathbf{x}, t) = \int_\Gamma \int_0^t \left[G(r, t-\tau) p(\xi, \tau) - \frac{\partial G}{\partial \mathbf{n}_\xi}(r, t-\tau) u(\xi, \tau) \right] d\tau \, d\gamma_\xi, \tag{5}$$

where $r = \|\mathbf{r}\|_2 = \|\mathbf{x} - \xi\|_2$ and

$$G(r, t-\tau) := \frac{1}{2\pi} \frac{H[t-\tau-r]}{\sqrt{[(t-\tau)^2 - r^2]}} \tag{6}$$

is the forward fundamental solution of the two dimensional wave operator, with $H[\,\cdot\,]$ the Heaviside function. With a limiting process for $\mathbf{x}$ tending to Γ we obtain the space-time BIE (see [27])

$$\frac{1}{2}\, u(\mathbf{x}, t) = \int_\Gamma \int_0^t G(r, t-\tau) p(\xi, \tau)\, d\tau \, d\gamma_\xi - \int_\Gamma \int_0^t \frac{\partial G}{\partial \mathbf{n}_\xi}(r, t-\tau) u(\xi, \tau)\, d\tau \, d\gamma_\xi\,, \tag{7}$$

which can be written, with obvious meaning of notation, in the compact form

$$\frac{1}{2}\, u(\mathbf{x}, t) = (Vp)(\mathbf{x}, t) - (Ku)(\mathbf{x}, t). \tag{8}$$

The BIE (8) is generally used to solve Dirichlet problem, but can be employed for mixed problems too. However, in this last case, we consider a second space-time BIE, obtainable from (5), performing the normal derivative with respect to $\mathbf{n}_\mathbf{x}$ and operating a limiting process for $\mathbf{x}$ tending to Γ we obtain

$$\frac{1}{2}\, p(\mathbf{x}, t) = \int_\Gamma \int_0^t \frac{\partial G}{\partial \mathbf{n}_\mathbf{x}}(r, t-\tau) p(\xi, \tau)\, d\tau \, d\gamma_\xi - \int_\Gamma \int_0^t \frac{\partial^2 G}{\partial \mathbf{n}_\mathbf{x}\, \partial \mathbf{n}_\xi}(r, t-\tau) u(\xi, \tau)\, d\tau d\gamma_\xi, \tag{9}$$

which can be written in the compact form

$$\frac{1}{2}\, p(\mathbf{x}, t) = (K' p)(\mathbf{x}, t) - (Du)(\mathbf{x}, t). \tag{10}$$

Note that the operator K' is the adjoint of the Cauchy singular operator K, which can be expressed as

$$Ku(\mathbf{x}, t) = -\int_\Gamma \frac{\partial r}{\partial \mathbf{n}_\xi} \int_0^t G(r, t-\tau) \left[u_t(\xi, \tau) + \frac{u(\xi, \tau)}{(t-\tau+r)} \right] d\tau \, d\gamma_\xi\,. \tag{11}$$

Expression (11) can be obtained starting from the definition of the double layer

operator K and observing that

$$\frac{\partial}{\partial r}\frac{H[t-\tau-r]}{\sqrt{t-\tau-r}}=\frac{\partial}{\partial \tau}\frac{H[t-\tau-r]}{\sqrt{t-\tau-r}}\,. \tag{12}$$

In fact, using (12) we have

$$\begin{aligned}\frac{\partial G}{\partial \mathbf{n}_\xi}(r,t-\tau)&=\frac{\partial G}{\partial r}(r,t-\tau)\,\frac{\partial r}{\partial \mathbf{n}_\xi}\\ &=\frac{1}{2\,\pi}\,\frac{\partial}{\partial r}\Big[\frac{1}{\sqrt{t-\tau+r}}\,\frac{H[t-\tau-r]}{\sqrt{t-\tau-r}}\Big]\,\frac{\partial r}{\partial \mathbf{n}_\xi}\\ =\frac{1}{2\,\pi}\,\Big[-\frac{1}{2}\,\frac{1}{t-\tau+r}\,\frac{H[t-\tau-r]}{\sqrt{(t-\tau)^2-r^2}}&+\frac{1}{\sqrt{t-\tau+r}}\,\frac{\partial}{\partial \tau}\,\frac{H[t-\tau-r]}{\sqrt{t-\tau-r}}\Big]\,\frac{\partial r}{\partial \mathbf{n}_\xi}\,.\end{aligned} \tag{13}$$

Now, inserting (13) in the definition of K, integrating in the sense of distributions the term containing the derivative with respect to τ, one gets, up to the factor $-1/(2\,\pi)$,

$$\int_\Gamma \frac{\partial r}{\partial \mathbf{n}_\xi}\int_0^t\Big[\frac{1}{2}\,\frac{H[t-\tau-r]}{\sqrt{(t-\tau)^2-r^2}}\frac{u(\xi,\tau)}{t-\tau+r}+\frac{H[t-\tau-r]}{\sqrt{t-\tau-r}}\,\frac{\partial}{\partial \tau}\Big[\frac{u(\xi,\tau)}{\sqrt{t-\tau+r}}\Big]\Big]d\tau d\gamma_\xi;$$

expressing explicitly the time derivative of the second term in the integrand function, one finally deduces (11).

Further, considering at this stage the derivative with respect to $\mathbf{n}_\mathbf{x}$ of (11) and operating with the same arguments as before, after a cumbersome but easy calculation the hypersingular integral operator D in (10) can be equivalently expressed in the following way

$$\begin{aligned}Du(\mathbf{x},t)=&-\int_\Gamma \frac{\partial^2 r}{\partial \mathbf{n}_\mathbf{x}\partial \mathbf{n}_\xi}\int_0^t G(r,t-\boldsymbol{\tau})\Big[u_t(\xi,\boldsymbol{\tau})+\frac{u(\xi,\boldsymbol{\tau})}{(t-\boldsymbol{\tau}+r)}\Big]\,d\boldsymbol{\tau}\,d\gamma_\xi\\ &+\int_\Gamma \frac{\partial r}{\partial \mathbf{n}_\mathbf{x}}\,\frac{\partial r}{\partial \mathbf{n}_\xi}\int_0^t G(r,t-\boldsymbol{\tau})\Big[u_{tt}(\xi,\boldsymbol{\tau})+\frac{2\,u_t(\xi,\boldsymbol{\tau})}{(t-\boldsymbol{\tau}+r)}+\frac{3\,u(\xi,\boldsymbol{\tau})}{(t-\boldsymbol{\tau}+r)^2}\Big]\,d\boldsymbol{\tau}\,d\gamma_\xi.\end{aligned}$$

Hence, using the boundary conditions (3)-(4), a mixed boundary value wave propagation problem can be rewritten as a system of two BIEs in the boundary unknowns the functions $p(\mathbf{x},t)$ and $u(\mathbf{x},t)$ on Γ_u, Γ_p, respectively

$$\begin{bmatrix} V_u & -K_p\\ -K'_u & D_p\end{bmatrix}\begin{bmatrix}p\\ u\end{bmatrix}=\begin{bmatrix} -V_p & \frac{1}{2}I+K_u\\ -\frac{1}{2}I+K'_p & -D_u\end{bmatrix}\begin{bmatrix}\bar{p}\\ \bar{u}\end{bmatrix},\ \begin{matrix}(\mathbf{x},t)\in \Sigma_T^u\\ (\mathbf{x},t)\in \Sigma_T^p\end{matrix}, \tag{14}$$

where the boundary integral operator subscripts $\beta=u,p$ define their restriction to Σ_T^u or Σ_T^p. Then, starting from the observation that the solution of (1)-(4) satisfies the

following energy identity

$$\mathcal{E}(u,T) := \frac{1}{2}\int_{\Omega}\left[u_t^2(\mathbf{x},T) + |\nabla u(\mathbf{x},T)|^2\right] d\mathbf{x} = \int_{\Gamma}\int_{0}^{T} u_t(\mathbf{x},t)\,\frac{\partial u}{\partial \mathbf{n}_{\mathbf{x}}}(\mathbf{x},t)\,dt\,d\gamma_{\mathbf{x}}$$

obtainable multiplying equation (1) by u_t and integrating by parts over $\Sigma_T := \Omega \times [0,T]$, and remembering (8) and (10), the energetic weak formulation of the system (14) is defined as [1]

$$\begin{cases} \langle (V_u p)_t, \psi\rangle_{L^2(\Sigma_T^u)} - \langle (K_p u)_t, \psi\rangle_{L^2(\Sigma_T^u)} = \langle f_t^u, \psi\rangle_{L^2(\Sigma_T^u)} \\ -\langle K_u' p, \eta_t\rangle_{L^2(\Sigma_T^p)} + \langle D_p u, \eta_t\rangle_{L^2(\Sigma_T^p)} = \langle f^p, \eta_t\rangle_{L^2(\Sigma_T^p)} \end{cases}, \tag{15}$$

where

$$f_t^u = -(V_p\,\bar{p})_t + \left((\tfrac{1}{2}I + K_u)\,\bar{u}\right)_t, \qquad f^p = \left(-\tfrac{1}{2}I + K_p'\right)\bar{p} - D_u\,\bar{u}$$

and $\psi(\mathbf{x},t)$, $\eta(\mathbf{x},t)$ are suitable test functions, belonging to the same functional space of $p(\mathbf{x},t)$, $u(\mathbf{x},t)$, respectively. The first equation in (14) has been derived with respect to time and projected with the $L^2(\Sigma_T^u)$ scalar product onto the space of functions approximating $p(\mathbf{x},t)$, while the second equation in (14) has been projected with the $L^2(\Sigma_T^p)$ onto the space of time derivative of functions approximating $u(\mathbf{x},t)$. The interest reader is refered to [7] for the appropriate functional setting. Note that the involved scalar products are represented by a space-time integral; hence, taking into account the space-time integral nature of operators V, K, K', D, in (15) we will have to deal with quadruple integrals, double in space and double in time.

2.1 - *Galerkin BEM discretization*

For time discretization we consider a uniform decomposition of the time interval $[0,T]$ with time step $\Delta t = T/N_{\Delta t}\,, N_{\Delta t} \in \mathbb{N}^+$, generated by the $N_{\Delta t}+1$ instants

$$t_k = k\,\Delta t, \quad k = 0, \cdots, N_{\Delta t}\,,$$

and we choose temporally piecewise constant shape functions for the approximation of p and piecewise linear shape functions for the approximation of u, although higher degree shape functions can be used. Note that, for this particular choice, temporal shape functions, for $k = 0, \cdots, N_{\Delta t} - 1$, will be defined as

$$v_k^p(t) = H[t - t_k] - H[t - t_{k+1}]\,, \qquad v_k^u(t) = R(t - t_k) - R(t - t_{k+1}),$$

[1] See also [4], where the energetic weak formulation was introduced for the problem (1)-(4) with domain $\Omega \subset \mathbb{R}$.

for the approximation of p and u, respectively, and $R(t-t_k)=\dfrac{t-t_k}{\Delta t}\,H[t-t_k]$ is the ramp function.

For the space discretization, we employ a Galerkin BEM. We consider a polygonal approximation of boundary $\Gamma=\Gamma_u\cup\Gamma_p$, denoted with $\widehat{\Gamma}=\widehat{\Gamma}_u\cup\widehat{\Gamma}_p$, where $\widehat{\Gamma}_u$ and $\widehat{\Gamma}_p$ are constituted by N_u, N_p straight elements $\{e_i^u\}_{i=1}^{N_u}$ and $\{e_i^p\}_{i=1}^{N_p}$, respectively; with $2l_i:=length(e_i^\beta)\le\Delta x$, $e_i^\beta\cap e_j^\beta=\emptyset$ if $i\neq j$ and $\beta=u,\,p$.

The functional background compels one to choose spatially shape functions belonging to $L^2(\widehat{\Gamma}_u)$ for the approximation of p and to $H_0^1(\widehat{\Gamma}_p)$ for the approximation of u. Hence, having defined $\mathcal{P}_{d_i}$ the space of algebraic polynomials of degree d_i on the element e_i of $\widehat{\Gamma}$, we consider, respectively, the space of piecewise polynomial functions

$$X_{\Delta x}^{-1}:=\{w^p(\mathbf{x})\in L^2(\widehat{\Gamma}_u):\ w^p_{|e_i^u}\in\mathcal{P}_{d_i}\,,\ \forall\, e_i^u\subset\widehat{\Gamma}_u\}\,; \tag{16}$$

and the space of continuous piecewise polynomial functions

$$X_{\Delta x}^{0}:=\{w^u(\mathbf{x})\in C^0(\widehat{\Gamma}_p):\ w^u_{|e_j^p}\in\mathcal{P}_{d_j}\,,\ \forall\, e_j^p\subset\widehat{\Gamma}_p\}\,. \tag{17}$$

Hence, denoting with M_u, M_p the number of unknowns on $\widehat{\Gamma}_u$ and $\widehat{\Gamma}_p$, respectively, and having introduced the standard piecewise polynomial boundary element basis functions $w_j^p(\mathbf{x})$, $j=1,\cdots,M_p$, in $X_{\Delta x}^{-1}$ and $w_j^u(\mathbf{x})$, $j=1,\cdots,M_u$ in $X_{\Delta x}^{0}$, the approximate solutions of the problem at hand will be expressed as

$$\tilde{p}(\mathbf{x},t):=\sum_{k=0}^{N_{\Delta t}-1}\sum_{j=1}^{M_p}\alpha_{pj}^{(k)}\,w_j^p(\mathbf{x})\,v_k^p(t),\quad \tilde{u}(\mathbf{x},t):=\sum_{k=0}^{N_{\Delta t}-1}\sum_{j=1}^{M_u}\alpha_{uj}^{(k)}\,w_j^u(\mathbf{x})\,v_k^u(t). \tag{18}$$

The Galerkin BEM discretization coming from energetic weak formulation (15) produces the linear system

$$\mathbb{E}\,\boldsymbol{\alpha}=\mathbf{b}\,, \tag{19}$$

where matrix $\mathbb{E}$ has a block lower triangular Toeplitz structure, since its elements depend on the difference t_h-t_k and in particular they vanish if $t_h\le t_k$. Each block has dimension $M:=M_p+M_u$. If we indicate with $\mathbb{E}^{(\ell)}$ the block obtained when $t_\ell:=t_h-t_k=(\ell+1)\Delta t,\ \ell=0,\dots,N_{\Delta t}-1$, the linear system can be written as

$$\begin{pmatrix}\mathbb{E}^{(0)} & 0 & 0 & \cdots & 0\\ \mathbb{E}^{(1)} & \mathbb{E}^{(0)} & 0 & \cdots & 0\\ \mathbb{E}^{(2)} & \mathbb{E}^{(1)} & \mathbb{E}^{(0)} & \cdots & 0\\ \cdots & \cdots & \cdots & \cdots & 0\\ \mathbb{E}^{(N_{\Delta t}-1)} & \mathbb{E}^{(N_{\Delta t}-2)} & \cdots & \mathbb{E}^{(1)} & \mathbb{E}^{(0)}\end{pmatrix}\begin{pmatrix}\boldsymbol{\alpha}^{(0)}\\ \boldsymbol{\alpha}^{(1)}\\ \boldsymbol{\alpha}^{(2)}\\ \vdots\\ \boldsymbol{\alpha}^{(N_{\Delta t}-1)}\end{pmatrix}=\begin{pmatrix}\mathbf{b}^{(0)}\\ \mathbf{b}^{(1)}\\ \mathbf{b}^{(2)}\\ \vdots\\ \mathbf{b}^{(N_{\Delta t}-1)}\end{pmatrix} \tag{20}$$

where

$$\boldsymbol{\alpha}^{(\ell)} = \left(\alpha_j^{(\ell)}\right), \qquad \mathbf{b}^{(\ell)} = \left(b_j^{(\ell)}\right), \qquad j = 1, \ldots, M. \tag{21}$$

Note that each block has a 2×2 block sub-structure of the type

$$\mathbb{E}^{(\ell)} = \begin{bmatrix} \mathbb{E}_{uu}^{(\ell)} & \mathbb{E}_{up}^{(\ell)} \\ \mathbb{E}_{pu}^{(\ell)} & \mathbb{E}_{pp}^{(\ell)} \end{bmatrix} \tag{22}$$

where diagonal sub-blocks have dimensions M_p, M_u, respectively, $\mathbb{E}_{pu}^{(\ell)} = (\mathbb{E}_{up}^{(\ell)})^\top$ and it holds

$$\boldsymbol{\alpha}^{(\ell)} = \left(\alpha_{p1}^{(\ell)}, \cdots, \alpha_{pM_p}^{(\ell)}, \alpha_{u1}^{(\ell)}, \cdots, \alpha_{uM_u}^{(\ell)}\right)^\top.$$

The solution of (20) is obtained with a block forward substitution, i.e. at every time instant t_ℓ, one computes

$$\mathbf{z}^{(\ell)} = \mathbf{b}^{(\ell)} - \sum_{j=1}^{\ell} \mathbb{E}^{(j)} \boldsymbol{\alpha}^{(\ell-j)}, \qquad \ell = 0, \cdots, N_{\Delta t} - 1\,,$$

and then solves the reduced linear system

$$\mathbb{E}^{(0)} \boldsymbol{\alpha}^{(\ell)} = \mathbf{z}^{(\ell)}\,. \tag{23}$$

Procedure (23) is a time-marching technique, where the only matrix to be inverted is the symmetric non-singular $\mathbb{E}^{(0)}$ diagonal block, while all the other blocks are used to update at every time step the right-hand side. Owing to this procedure we can construct and store only the blocks $\mathbb{E}^{(0)}, \cdots, \mathbb{E}^{(N_{\Delta t}-1)}$ with a considerable reduction of computational cost and memory requirement.

Having set $\Delta_{hk} = t_h - t_k$, the matrix elements in blocks of the type $\mathbb{E}_{uu}^{(\ell)}$, after a double analytic integration in the time variables, are of the form

$$\sum_{\alpha,\beta=0}^{1} (-1)^{\alpha+\beta} \int_{\widehat{\Gamma}_u} w_i^p(\mathbf{x}) \int_{\widehat{\Gamma}_u} H[\Delta_{h+\alpha,k+\beta} - r]\, \mathcal{V}(r, t_{h+\alpha}, t_{k+\beta})\, w_j^p(\boldsymbol{\xi})\, d\gamma_{\boldsymbol{\xi}}\, d\gamma_{\mathbf{x}}, \tag{24}$$

where

$$\mathcal{V}(r, t_h, t_k) = \frac{1}{2\pi}\left[\log\left(\Delta_{hk} + \sqrt{\Delta_{hk}^2 - r^2}\right) - \log\, r\right]; \tag{25}$$

matrix elements in blocks of the type $\mathbb{E}_{up}^{(\ell)}$, after a double analytic integration in the

time variables, are of the form

$$\sum_{\alpha,\beta=0}^{1}(-1)^{\alpha+\beta}\int\limits_{\widehat{\Gamma}_u} w_i^p(\mathbf{x})\int\limits_{\widehat{\Gamma}_p} H[\Delta_{h+\alpha,k+\beta}-r]\,\mathcal{K}(r,t_{h+\alpha},t_{k+\beta})\,w_j^u(\boldsymbol{\xi})\,d\gamma_{\boldsymbol{\xi}}d\gamma_{\mathbf{x}}, \tag{26}$$

where

$$\mathcal{K}(r,t_h,t_k)=\frac{1}{2\pi\Delta t}\,\frac{\mathbf{r}\cdot\mathbf{n}_{\boldsymbol{\xi}}}{r^2}\,\sqrt{\Delta_{hk}^2-r^2}\,; \tag{27}$$

matrix elements in blocks of the type $\mathbb{E}_{pp}^{(\ell)}$, after a double analytic integration in the time variables, are of the form

$$\sum_{\alpha,\beta=0}^{1}(-1)^{\alpha+\beta}\int\limits_{\widehat{\Gamma}_p} w_i^u(\mathbf{x})\int\limits_{\widehat{\Gamma}_p} H[\Delta_{h+\alpha,k+\beta}-r]\,\mathcal{D}(r,t_{h+\alpha},t_{k+\beta})\,w_j^u(\boldsymbol{\xi})\,d\gamma_{\boldsymbol{\xi}}d\gamma_{\mathbf{x}}, \tag{28}$$

where

$$\begin{aligned}\mathcal{D}(r,t_h,t_k)=&\frac{1}{2\pi(\Delta t)^2}\Big\{\frac{(\mathbf{r}\cdot\mathbf{n}_{\mathbf{x}})(\mathbf{r}\cdot\mathbf{n}_{\boldsymbol{\xi}})}{r^2}\,\frac{\Delta_{hk}\sqrt{\Delta_{hk}^2-r^2}}{r^2}\\&+\frac{(\mathbf{n}_{\mathbf{x}}\cdot\mathbf{n}_{\boldsymbol{\xi}})}{2}\Big[\log(\Delta_{hk}+\sqrt{\Delta_{hk}^2-r^2})-\log r-\frac{\Delta_{hk}\sqrt{\Delta_{hk}^2-r^2}}{r^2}\Big]\Big\}.\end{aligned} \tag{29}$$

We will refer to one of the double integrals in (24), (26) or (28), in the sequel indicated by

$$\int\limits_{\widehat{\Gamma}_\alpha} w_i(\mathbf{x})\int\limits_{\widehat{\Gamma}_\beta} H[\Delta_{hk}-r]\,\mathcal{S}(r,t_h,t_k)\,w_j(\boldsymbol{\xi})\,d\gamma_{\boldsymbol{\xi}}\,d\gamma_{\mathbf{x}}\,, \tag{30}$$

where $\alpha,\ \beta=u,\ p$ and $\mathcal{S}$ represents one of the kernels (25), (27) or (29) and where we have dropped redundant apices u,p in the notation, being clear which parts of the boundary and which test and shape functions are involved in the double integration, in relation to the fixed kernel. In the following, this simplification will be operated whenever possible.

Using the standard element by element technique, the evaluation of every double integral of the form (30) is reduced to the assembling of local contributions of the type

$$\int_0^{2l_i}\tilde{w}_m^{(d_i)}(s)\int_0^{2l_j} H[\Delta_{hk}-r]\,\mathcal{S}(r,t_h,t_k)\,\tilde{w}_n^{(d_j)}(z)\,dz\,ds\,, \tag{31}$$

where $\tilde{w}_m^{(d_i)}, m = 0, \cdots, d_i$ ($\tilde{w}_n^{(d_j)}, n = 0, \cdots, d_j$) defines one of the local lagrangian basis function in the space variable of degree d_i (d_j) defined over the element e_i (e_j) of the boundary mesh.

Looking at (25), (27) and (29), we observe space singularities of type $\log r$, $O(r^{-1})$ and $O(r^{-2})$ as $r \to 0$, which are typical of $2D$ static weakly singular, singular and hypersingular kernels. Hence, efficient evaluation of double integrals of type (31) is particularly required when $e_i \equiv e_j$ and when $e_i\,, e_j$ are consecutive. Note that when the kernel is hypersingular and $e_i \equiv e_j$ we define both the inner and the outer integrals as Hadamard finite parts [**19**], while if e_i and e_j are consecutive, only the outer integral is understood in the finite part sense: the correct interpretation of double integrals is the key point for any efficient numerical approach based on element by element technique (see [**3**]).

Further, we observe that the Heaviside function $H[\Delta_{hk} - r]$ in (31) and the function $\sqrt{\Delta_{hk}^2 - r^2}$ in the kernel $\mathcal{S}(r, t_h, t_k)$, give rise to other different type of troubles, which have to be properly faced, as described in [**6**]. Hence, the numerical treatment of (31) has been operated through quadrature schemes widely used in the context of Galerkin BEM coming from elliptic problems [**3**], coupled with a suitable regularization technique [**31**], after a careful subdivision of the integration domain due to the presence of the Heaviside function. In the following sections we present a complete list of efficient numerical integration schemes we have used for the discretization of weakly, strongly and hypersingular BIEs related to wave propagation problems and which represent a valid alternative to those proposed in [**17, 38**].

3 - Evaluation of Galerkin matrix elements

Let us start with an analysis of the double integration domain in (31). Due to the presence of the Heaviside function $H[\Delta_{hk} - r]$, the double integration domain is constituted by the intersection between the rectangle $[0, 2\,l_i] \times [0, 2\,l_j]$ and the 2D domain $\Delta_{hk} - r > 0$. Let us specify this issue with respect to the geometrical disposition of the mesh elements e_i and e_j.

Coincident boundary elements ($e_i \equiv e_j$)

In this case, the distance between the source and the field point can be written as $r = |s - z|$; hence the double integration domain is represented by the intersection between the square $[0, 2\,l_i] \times [0, 2\,l_i]$ and the strip $|s - z| < \Delta_{hk}$ where

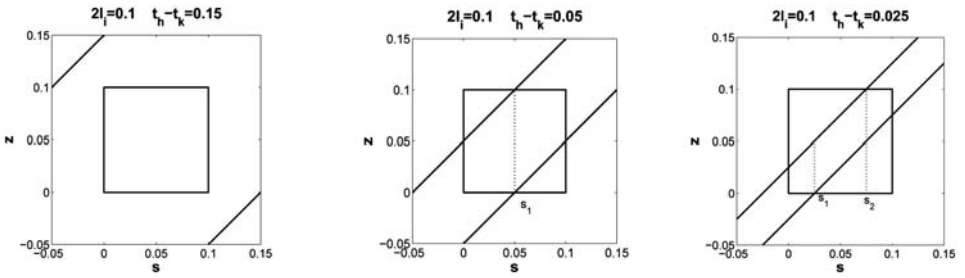

Fig. 1. Double integration domain (coincident elements) for different values of Δ_{hk}.

the Heaviside function is not trivial. In Figure 1 we show these intersections for different values of Δ_{hk} and fixed length $2l_i$. Having set

$$M_s = \max(0, s - \Delta_{hk}), \qquad m_s = \min(2l_i, s + \Delta_{hk}),$$

double integral (31) in this case becomes

$$\int_0^{2l_i} \tilde{w}_m^{(d_i)}(s) \int_{M_s}^{m_s} \mathcal{S}(r, t_h, t_k)\, \tilde{w}_n^{(d_i)}(z)\, dz\, ds\,. \tag{32}$$

The numerical quadrature in the outer variable of integration s has been performed subdividing, when necessary, the outer interval of integration. Without this subdivision, one should use a lot of quadrature nodes for the outer numerical integration in order to achieve the single precision accuracy. Let us explain this issue in details. The derivative with respect to s of the outer integrand function, after the inner integration, presents jumps in correspondence to possible subdivision points given by

$$s_1 = \Delta_{hk}, \qquad s_2 = 2l_i - \Delta_{hk}\,.$$

Note that in this simple geometrical case, if $\Delta_{hk} > 2l_i$ these points do not belong to the integration interval $[0, 2l_i]$; if $\Delta_{hk} = 2l_i$ these points coincide with the endpoints of the integration interval $[0, 2l_i]$; when $0 < \Delta_{hk} < 2l_i$, $\Delta_{hk} \neq l_i$ both points belong to $[0, 2l_i]$; at last, when $\Delta_{hk} = l_i$ only one point belongs to the integration interval ($s_1 = s_2$). Almost all these geometrical situations as shown in Figure 1. Further, as an example, in Figure 2 we present the behavior of the derivative

$$\frac{d}{ds}\left[\int_{M_s}^{m_s} \log\left(\Delta_{hk} + \sqrt{\Delta_{hk}^2 - |s - z|^2}\right) \tilde{w}_j^{(0)}(z)\, dz\right],$$

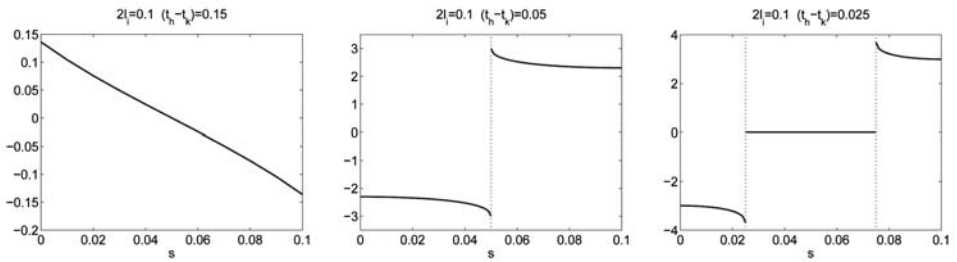

Fig. 2. Behavior of outer integrand function derivative for different values of Δ_{hk}.

referred to the domains of the previous figure and to an integrand function related to the non-singular (for $r \to 0$) part of the kernel (29).

Hence, (32) will be eventually decomposed into the sum of double integrals of the form

$$\int_a^b \tilde{w}_m^{(d_i)}(s) \int_{M_s}^{m_s} \mathcal{S}(r, t_h, t_k)\, \tilde{w}_n^{(d_i)}(z)\, dz\, ds\,, \tag{33}$$

where $[a, b] \subset [0, 2l_i]$. Of course when no subdivision is needed, we will have to deal with only one double integral (33) where $[a, b] \equiv [0, 2l_i]$.

In Table 1 the computational gain obtained to achieve single precision accuracy when using the suggested splitting is displayed in the numerical evaluation of the

Table 1. *Relative errors in the outer numerical integration of* (34) *when* $\Delta_{hk} = 0.05, 0.025$*, with and without the proposed splitting. The symbol* $--$ *means that the single precision accuracy has been achieved.*

	$\Delta_{hk} = 0.05$		$\Delta_{hk} = 0.025$	
n. nodes	without splitting	with splitting	without splitting	with splitting
4	$1.5871 \cdot 10^{-2}$	$1.2663 \cdot 10^{-5}$	$4.8220 \cdot 10^{-4}$	$4.7584 \cdot 10^{-6}$
8	$4.4374 \cdot 10^{-3}$	$4.8539 \cdot 10^{-7}$	$5.2265 \cdot 10^{-2}$	$7.3393 \cdot 10^{-7}$
16	$1.1928 \cdot 10^{-3}$	$--$	$2.1787 \cdot 10^{-4}$	$--$
32	$3.1162 \cdot 10^{-4}$		$3.9416 \cdot 10^{-4}$	
64	$7.9969 \cdot 10^{-5}$		$2.1043 \cdot 10^{-5}$	
128	$2.0301 \cdot 10^{-5}$		$2.5823 \cdot 10^{-5}$	
256	$5.1162 \cdot 10^{-6}$		$2.0254 \cdot 10^{-6}$	
512	$1.2786 \cdot 10^{-6}$		$1.1237 \cdot 10^{-6}$	
1024	$3.1285 \cdot 10^{-7}$		$6.6507 \cdot 10^{-7}$	
2048	$--$		$--$	

outer integral of

$$I = \int_0^{2l_i} \int_{M_s}^{m_s} \log\left(\Delta_{hk} + \sqrt{\Delta_{hk}^2 - |s-z|^2}\right) dz\, ds\,, \tag{34}$$

for $2l_i = 0.1$ and $\Delta_{hk} = 0.05,\ 0.025$, using a classical Gauss-Legendre rule. In this simple geometrical case, the inner integral has been evaluated analytically.

Consecutive aligned boundary elements ($e_j \equiv e_{i+1}$)

In this case, the distance between the source and the field point can be written as $r = s + z$, with $s \in [0, 2l_i]$ and $z \in [0, 2l_j]$. Hence the double integration domain is represented by the intersection between the rectangle $[0, 2\,l_i] \times [0, 2\,l_j]$ and the half plane: $z < \Delta_{hk} - s$, where the Heaviside function is not trivial. This intersection will be not empty if: $0 < s < \Delta_{hk}$. Therefore, having set

$$m_0 = \min\left(\Delta_{hk}, 2l_i\right), \qquad m_s = \min\left(2l_j, \Delta_{hk} - s\right),$$

double integral (31) in this case becomes

$$\int_0^{m_0} \tilde{w}_m^{(d_i)}(s) \int_0^{m_s} \mathcal{S}(r, t_h, t_k)\, \tilde{w}_n^{(d_j)}(z)\, dz\, ds\,. \tag{35}$$

Also in this case, the numerical quadrature in the outer variable of integration s has been performed subdividing, when necessary, the outer interval of integration. In fact, the derivative with respect to s of the outer integrand function, after the inner integration, presents a jump in correspondence to a possible subdivision point given by

$$s_1 = \Delta_{hk} - 2l_j\,.$$

Note that in this geometrical case, it is simple to verify that if $\Delta_{hk} < 2l_j$ or $\Delta_{hk} > 2l_i + 2l_j$ this point does not belong to the integration interval $[0, m_0]$, while if $2l_j + 2l_i < \Delta_{hk} < 2l_j$, s_1 breaks in two subintervals the outer integration interval $[0, m_0]$. Hence, (35) will be eventually decomposed into the sum of double integrals of the form

$$\int_a^b \tilde{w}_i^{(d_i)}(s) \int_0^{m_s} \mathcal{S}(r, t_h, t_k)\, \tilde{w}_{i+1}^{(d_{i+1})}(z)\, dz\, ds\,, \tag{36}$$

where $[a, b] \subset [0, m_0]$. Of course when no subdivision is needed, we will have to deal with only one double integral (36) where $[a, b] \equiv [0, m_0]$.

Consecutive not aligned boundary elements ($e_j \equiv e_{i+1}$)

In this case, having set $\omega = \alpha + \beta$ (see Figure 3), the distance between the source and the field point can be written as: $r = [z^2 + 2\,sz\cos\omega + s^2]^{1/2}$, with $s \in [0, 2l_i]$, $z \in [0, 2l_{i+1}]$ and $0 < \omega < \pi$. Hence the double integration domain is represented by the intersection between the rectangle $[0, 2\,l_i] \times [0, 2\,l_j]$ and the ellipsis $r^2 - \Delta_{hk}^2 < 0$ centered in the unique singularity point $(0, 0)$, where the Heaviside function is not trivial.

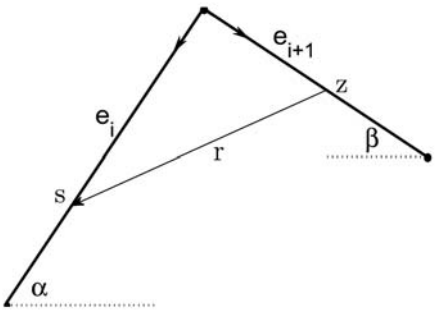

Fig. 3. Geometrical representation of consecutive not aligned elements.

The directions of the two axes of the ellipsis are $(-1, 1)$ and $(1, 1)$ with semi-length respectively $(1 - \cos\omega)^{-1/2}$ and $(1 + \cos\omega)^{-1/2}$. Of course, when $0 < \cos\omega < 1$ the major axis will be oriented in direction $(1, 1)$, when $-1 < \cos\omega < 0$ the major axis will be oriented in direction $(-1, 1)$, when $\cos\omega = 0$ the ellipsis becomes a circle. The angle $\theta = \pi - \omega$ between contiguous elements determines the eccentricity, while the increasing parameter Δ_{hk} determines a dilation of the ellipsis. In Figure 4, we show various types of intersections, i.e. double integration domains, for different values of Δ_{hk} and different angles θ between contiguous elements. Note that the inequality

$$z^2 + 2\,sz\cos\omega + s^2 - \Delta_{hk}^2 < 0\,, \tag{37}$$

can be satisfied if and only if

$$\Delta_{hk}^2 - s^2\sin^2\omega > 0 \quad \Leftrightarrow \quad -\frac{\Delta_{hk}}{\sin\omega} < s < \frac{\Delta_{hk}}{\sin\omega}\,.$$

For $s \in (0, 2l_i)$ the lower limitation for the outer variable of integration is always satisfied; then under the restrictions: $0 < s < \Delta_{hk}/\sin\omega$, the inequality (37) will be satisfied for

$$z_1^s < z < z_2^s\,, \quad \text{where} \quad z_{1,2}^s = -s\cos\omega \mp \sqrt{\Delta_{hk}^2 - s^2\sin^2\omega}.$$

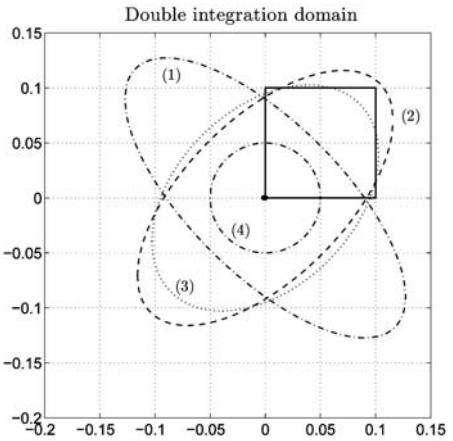

Fig. 4. Double integration domain (consecutive not aligned boundary elements of length $2l_i = 2l_j = 0.1$) for different values of Δ_{hk} and angles ω: (1) $\Delta_{hk} = 0.09, \omega = \pi/4$, (2) $\Delta_{hk} = 0.095, \omega = 5\pi/8$, (3) $\Delta_{hk} = 0.092, \omega = 17\pi/24$, (4) $\Delta_{hk} = 0.05, \omega = \pi/2$.

Therefore, having set

$$m_0 = \min\,(2l_i, \frac{\Delta_{hk}}{\sin\omega}), \qquad M_s = \max\,(0, z_1^s), \qquad m_s = \min\,(2l_j, z_2^s)\,,$$

double integral (31) in this case becomes

$$\int_0^{m_0} \tilde{w}_m^{(d_i)}(s) \int_{M_s}^{m_s} \mathcal{S}(r, t_h, t_k)\, \tilde{w}_n^{(d_j)}(z)\, dz\, ds\,. \tag{38}$$

The numerical quadrature in the outer variable of integration s has been performed subdividing, when necessary, the outer interval of integration. In fact, also in this case, the derivative with respect to s of the outer integrand function, after the inner integration, presents a jump in correspondence to possible subdivision points to be searched among the solutions of the equations

$$z_1^s = 0, \qquad z_2^s = 2l_j\,,$$

formally given by

$$s_1^{1,2} = \mp\Delta_{hk}, \qquad s_2^{1,2} = -2l_j\cos\omega \mp \sqrt{\Delta_{hk}^2 - (2l_j)^2\sin^2\omega}\,.$$

Note that $s_1^1 = -\Delta_{hk} \notin [0, m_0]$ and we can write real solutions $s_2^{1,2}$ under the restriction: $\Delta_{hk} > 2l_j\sin\omega$. Having set

$$\ell_\omega^2 = (2l_i)^2 + (2l_j)^2 + 2(2l_i)(2l_j)\cos\omega\,,$$

with a deeper analysis, one obtains that:

- $s_1^2 \in [0, m_0]$ when $0 < \Delta_{hk} < 2l_i$;
- for $0 < \omega < \pi/2$

only s_2^2 breaks the outer integration interval $[0, m_0]$ in two subintervals when: $2l_j < \Delta_{hk} < \ell_\omega$;

- for $\pi/2 < \omega < \pi$
  - if $\cos\omega > -2l_i/2l_j$
    $s_2^2 \in [0, m_0]$ when $2l_j \sin\omega < \Delta_{hk} < \ell_\omega$,
  - if $\cos\omega > -2l_i/2l_j$
    $s_2^1 \in [0, m_0]$ when $2l_j \sin\omega < \Delta_{hk} < 2l_j$,
    otherwise when $\max\{2l_j \sin\omega, \ell_\omega\} < \Delta_{hk} < 2l_j$.

Hence, the integral (38) will be eventually decomposed into the sum of double integrals of the form

$$\int_a^b \tilde{w}_m^{(d_i)}(s) \int_{M_s}^{m_s} \mathcal{S}(r, t_h, t_k)\, \tilde{w}_n^{(d_j)}(z)\, dz\, ds\,, \tag{39}$$

where $[a, b] \subset [0, m_0]$. Of course, when no subdivision is needed, we will have to deal with only one double integral (39) where $[a, b] \equiv [0, m_0]$. Note that for some values of s it could happen that $m_s - M_s \leq 0$; in this case the inner integral does not give any contribution to the final result and its evaluation has to be avoided.

Disjoint elements ($\bar{e}_i \cap \bar{e}_j = \emptyset$)

Having indicated with (x_{i-1}^1, x_{i-1}^2), (x_i^1, x_i^2) the end-points of e_i and with $(\xi_{j-1}^1, \xi_{j-1}^2)$, (ξ_j^1, ξ_j^2) the end-points of e_j, the distance between the source and the field points can be written as

$$r = \left[[a + b\,s - c\,z]^2 + [d + e\,s - f\,z]^2\right]^{1/2},$$

where

$$a = x_{i-1}^1 - \xi_{j-1}^1, \quad b = \frac{x_i^1 - x_{i-1}^1}{2l_i}, \quad c = \frac{\xi_j^1 - \xi_{j-1}^1}{2l_j},$$
$$d = x_{i-1}^2 - \xi_{j-1}^2 \quad e = \frac{x_i^2 - x_{i-1}^2}{2l_i}, \quad f = \frac{\xi_j^2 - \xi_{j-1}^2}{2l_j}.$$

The double integration domain is the intersection between the rectangle $[0, 2l_i] \times [0, 2l_j]$ and the 2D domain:

$$r < \Delta_{hk} \qquad \Leftrightarrow \qquad [a + b\,s - c\,z]^2 + [d + e\,s - f\,z]^2 < \Delta_{hk}^2, \tag{40}$$

where the Heaviside function is not trivial. Using the relations

$$b^2 + e^2 = 1\,, \qquad c^2 + f^2 = 1\,,$$

with a straightforward calculation, we obtain that the inequality (40) is satisfied if and only if

$$\Delta_{hk}^2 - ((bf - ce)s + af - cd)^2 > 0,$$

that implies restriction on the outer variable of integration s when $bf - ce \neq 0$; more precisely:

$$\text{if } \; bf - ce > 0 \qquad m := \frac{-\Delta_{hk} - (af - cd)}{bf - ce} < s < \frac{\Delta_{hk} - (af - cd)}{bf - ce} =: M\,,$$

$$\text{if } \; bf - ce < 0 \qquad m := \frac{\Delta_{hk} - (af - cd)}{bf - ce} < s < \frac{-\Delta_{hk} - (af - cd)}{bf - ce} =: M\,.$$

Under these restrictions, the inequality (40) will be satisfied for

$$z_1^s < z < z_2^s,$$

where

$$z_{1,2}^s = (ac + df) + (bc + ef)s \mp \sqrt{\Delta_{hk}^2 - ((bf - ce)s + af - cd)^2}. \tag{41}$$

Therefore, having set

$$M_1 = \max(0, m), \qquad m_1 = \min(2l_i, M),$$

$$M_s = \max(0, z_1^s), \qquad m_s = \min(2l_j, z_2^s),$$

double integral (31) in this case becomes

$$\int_{M_1}^{m_1} \tilde{w}_m^{(d_i)}(s) \int_{M_s}^{m_s} \mathcal{S}(r, t_h, t_k)\, \tilde{w}_n^{(d_j)}(z)\, dz\, ds\,. \tag{42}$$

The numerical quadrature in the outer variable of integration s has been optimally performed subdividing, when necessary, the outer interval of integration. In fact, the derivative with respect to s of the outer integrand function, after the inner integration, presents a jump in correspondence to possible subdivision points to be

searched among the solutions of the equations

$$z_1^s = 0, \qquad z_2^s = 2l_j,$$

formally given by

$$s_1^{1,2} = \beta_1 \mp \sqrt{\Delta_{hk}^2 + \lambda_1}\,, \qquad s_2^{1,2} = \beta_2 \mp \sqrt{\lambda_2 - \Delta_{hk}^2}\,,$$

with:

$$\begin{aligned} &\beta_1 = -(ab + de), && \lambda_1 = (ab + de)^2 - a^2 - d^2\,, \\ &\beta_2 = 2l_j(bc + ef) - (ab + de)\,, && \lambda_2 = a^2 + d^2 - 2l_j(ac + df - 2l_j). \end{aligned}$$

When one or more of these solutions are real and belong to the outer interval of integration, (42) will be decomposed into the sum of double integrals of the form

$$\int_a^b \tilde{w}_m^{(d_i)}(s) \int_{M_s}^{m_s} \mathcal{S}(r, t_h, t_k)\, \tilde{w}_n^{(d_j)}(z)\, dz\, ds\,, \tag{43}$$

where $[a, b] \subset [M_1, m_1]$. Without this subdivision, one should use a lot of quadrature nodes for the outer numerical integration in order to achieve the single precision accuracy. Of course, when no subdivision is needed, we will have to deal with only one double integral (43) where $[a, b] \equiv [M_1, m_1]$. Note that for some values of s it could happen that $m_s - M_s \leq 0$: in this case the inner integral does not give any contribution to the final result and its evaluation has to be avoided.

4 - Basic quadrature rules

A quadrature formula widely used to generate Galerkin matrix elements is a rule introduced in [**31**], that efficiently integrates functions with weak singularities at the end-points of the integration interval. In fact classical Gauss-Legendre formula

$$\int_{-1}^{1} f(x)\, dx = \sum_{k=1}^{n} \lambda_k f(x_k) \; + \; R_n(f) \tag{44}$$

is very accurate for regular integrands, but looses its efficiency in presence of mild singularities of the integrand functions. Indeed, given any $f \in C^m[-1, +1]$ we have, for example, $R_n(f) = o(1)$ when $m = 0$ and $R_n(f) = O(n^{-m})$ otherwise. We will however show that, using very elementary tools, with this rule we can also easily handle several other cases where the function $f(x)$ is not smooth at all.

Now, let us consider an integral of the form $\int_0^1 f(s)ds$ where $f(s)$ presents weak singularities at the end-points of the integration interval. If we introduce a change of variable $s = \varphi(\tilde{s})$ mapping $(0,1)$ onto itself, with $\varphi'(\tilde{s}) \geq 0$, we obtain

$$\int_0^1 f(s)ds = \int_0^1 f(\varphi(\tilde{s}))\varphi'(\tilde{s})d\tilde{s} \equiv \int_0^1 F(\tilde{s})d\tilde{s}. \tag{45}$$

Further if

$$\varphi^{(i)}(0) = 0, \quad \varphi^{(j)}(1) = 0, \quad i = 1, \ldots, p-1, \quad j = 1, \ldots, q-1 \tag{46}$$

we can make function $F(\tilde{s})$ in (45) as smooth as we like, simply choosing integers p, q sufficiently large, and then we can use for the last integral in (45) the Gauss-Legendre rule. In the following we will consider the transformation proposed in [**31**]

$$\varphi(\tilde{s}) = \frac{(p+q-1)!}{(p-1)!(q-1)!} \int_0^{\tilde{s}} u^{p-1}(1-u)^{q-1}du, \qquad p, q \geq 1. \tag{47}$$

Integral in (47), with $n = \lfloor \frac{p+q}{2} \rfloor$, can be efficiently evaluated by a $n-$points Gauss-Legendre formula[2]. Then, if we apply the n-point Gauss-Legendre rule to the final form of (45) we obtain

$$\int_{-1}^{1} f(x)\,dx = \sum_{i=1}^{n} \lambda_i f(\varphi(x_i))\varphi'(x_i) + R_n(F)\,. \tag{48}$$

For this formula, with $p = 1$, we have the following convergence result (see [**32**]).

Theorem 4.1. *If $f(x) = (1-x)^m \log(1-x)$, with $m \in \mathbb{N}$, then we have*

$$R_n(F) = O(n^{2q(m+1)} \log n)\,. \tag{49}$$

This smoothing procedure has been actually generalized to integrals (44) with $f(x)$ having also a fixed number of internal weak singularities (see [**31**]).

In the following section, we will use certain product quadrature rules of interpolatory type, based on the zeros of Legendre polynomials. They are of the form

$$\int_{-1}^{1} S(y,x)f(x)\,\mathrm{d}x = \sum_{k=1}^{n} w_k(y)f(x_k) + R_n(f;y)\,, \tag{50}$$

---

[2] Here and in the sequel $\lfloor x \rfloor$ denotes the greatest integer less then or equal to x, while $\lceil x \rceil$ denotes the smallest integer greater then or equal to x.

and are obtained by replacing $f(x)$ by its Lagrange polynomial, of degree $n-1$, associated with the zeros $\{x_k\}$ of the Legendre polynomial $P_n(x)$, of degree n [**36**]. For the coefficients $\{w_k\}$ the following expression can be easily derived [**14**]

$$w_k(y) = \frac{1}{2}\lambda_k \sum_{i=0}^{n-1} (2i+1)\mu_i(y)P_i(x_k)\,, \tag{51}$$

where $\{\lambda_k\}$ denote the classical Christoffel numbers associated with the n-point Gauss-Legendre formula (44) and $P_i(x)$ is the $i-th$ degree Legendre polynomial, and $\mu_i(y)$ is the so-called *modified moment* of the kernel $S(y,x)$

$$\mu_i(y) = \int_{-1}^{1} S(y,x)P_i(x)\,\mathrm{d}x. \tag{52}$$

The rule (50) has degree of exactness $n-1$, i.e. it is exact whenever $f(x)$ is a polynomial of degree $n-1$. Expression (51) reduces the evaluation of $w_k(y)$ to the knowledge of modified moments recurrence relationships which stem from the well-known three-term recurrence satisfied by Legendre polynomials [**36**]. The kernels $S(y,x)$ of interest in this paper are: $\ln(\mid x-a_y \mid)$, $\ln[(x-a_y)^2+b_y^2]$, with $b_y \neq 0$, rational function containing factors of the type $(x-a_y)$, divisors of the type $(x-a_y)$ and $[(x-a_y)^2+b_y^2]$. For these kernels, recurrence relations giving (52) are shown in [**3**].

The next rule we need to consider is

$$\text{⨍}_0^1 \frac{f(s)}{s}\,\mathrm{d}s = w_0^{GR} f(0) + \sum_{k=1}^{n} w_k^{GR} f(s_k^{GR}) + R_n^{GR}(f) \tag{53}$$

$$s_k^{GR} = \frac{1+x_k}{2}\,, \qquad w_k^{GR} = \frac{\lambda_k}{2s_k} \quad k=1,\ldots,n\,, \qquad w_0^{GR} = -\sum_{k=1}^{n} w_k^{GR},$$

where $\{s_k^{GR}\}$ denote the Legendre zeros $\{x_k\}$ mapped on the interval $(0,1)$ and the integral is defined in the finite-part sense (see [**30**]). This rule is obtained by replacing $f(x)$ by its $n-th$ degree interpolation polynomial associated with the nodes $\{0, s_1, \ldots, s_n\}$. It is a Gauss-Radau type quadrature formula, i.e. it is exact whenever $f(x)$ is a polynomial of degree $\leq 2n$ and has the convergence property stated in the next theorem proved in [**30**].

Theorem 4.2. *Let be H_μ the space of Hölder continuous functions of order μ, if $f(x) \in C^p[0,1], p \geq 1$, with $f^{(p)} \in H_\mu[0,1]$, for some $0<\mu\leq 1$. Then*

$$R_n^{GR}(f) = O(n^{-p-\mu})\,.$$

5 - Numerical integration schemes

Looking at (25), (27) and (29), we will have here to consider, up to suitable constants, the numerical treatment of kernels of the type

$$\log r, \qquad \frac{\mathbf{r}\cdot\mathbf{n}_\xi}{r^2}\sqrt{\Delta_{hk}^2 - r^2}, \qquad \left[\frac{(\mathbf{r}\cdot\mathbf{n}_\mathbf{x})(\mathbf{r}\cdot\mathbf{n}_\xi)}{r^2} - \frac{\mathbf{n}_\mathbf{x}\cdot\mathbf{n}_\xi}{2}\right]\frac{\sqrt{\Delta_{hk}^2 - r^2}}{r^2}, \tag{54}$$

which present weak, Cauchy type and hyper singularities respectively when $r \to 0$. Hence these types of singularities arise in the double integration over coincident or adjacent boundary elements, while they haven't to be considered on a couple of disjoint elements.

Before going into the details of numerical quadrature schemes we have used to integrate these kernels, we observe that in (25) and (29) there is also another function, i.e. $\log(\Delta_{hk} + \sqrt{\Delta_{hk}^2 - r^2})$ which of course is not singular for $r \to 0$; nevertheless the inner numerical integration of this function has to be performed carefully even on couples of disjoint elements, when the boundary of the 2D region $r < \Delta_{hk}$, where the Heaviside function is not trivial, is contained in the rectangle $[0, 2l_i] \times [0, 2l_j]$.

The problem we have to deal with is due to the presence of the square root function $\sqrt{\Delta_{hk}^2 - r^2}$. We will illustrate this issue for the case of the double integration over a couple of coincident elements $e_i \equiv e_j$ of length $2l_i$, where $r = |s - z|$ in the local variables of integration $s, z \in (0, 2l_i)$. The argument of $\sqrt{\Delta_{hk}^2 - |s-z|^2}$ is always positive but it can assume very small values and in the limit for the argument tending to zero the derivative of the square root with respect to the inner variable of integration z becomes unbounded. This behavior happens along the oblique boundary of the double integration domain, as shown in Figure 1 for $\Delta_{hk} = 0.05,\ 0.025$, and produces a bad performance, for instance, even in the inner numerical integration of

$$\int_0^{2l_i}\int_{M_s}^{m_s} \log\left(\Delta_{hk} + \sqrt{\Delta_{hk}^2 - |s-z|^2}\right) dz\, ds\,, \tag{55}$$

with a classical Gauss-Legendre quadrature formula, in the sense that one should use a lot of quadrature nodes to achieve the single precision accuracy. To overcome this difficulty, we have considered, for the inner integration, the regularization procedure (45), which suitably pushes the Gaussian nodes towards the endpoints of the interval $[M_s, m_s]$ and modifies the Gaussian weights in order to regularize integrand functions with mild boundary singularities. The outer integral in (55) is performed with a classical Gauss-Legendre rule.

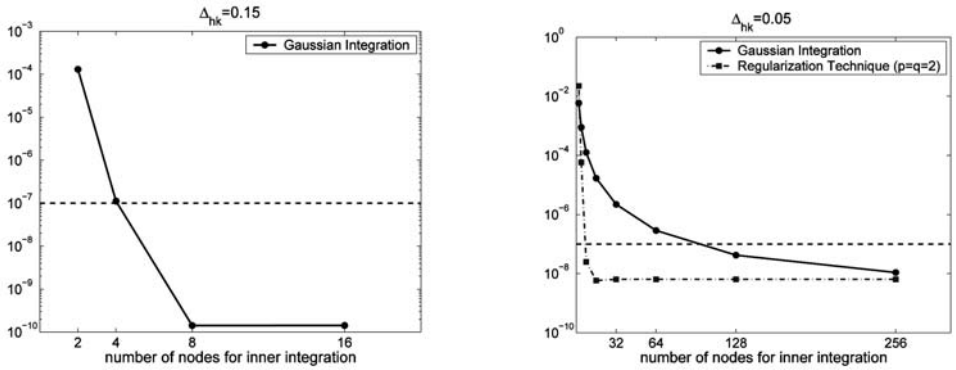

Fig. 5. Comparison between computational costs of Gaussian Quadrature and Regularization Procedure for the inner numerical integration of (55).

In Figure 5, we show the computational cost of the Gaussian quadrature formula and of the regularization procedure just explained in relation to the achievement of the single precision accuracy (horizontal line) in the evaluation of the double integral (55) for $2l_i = 0.1$ and $\Delta_{hk} = 0.15, 0.05$ (results for $\Delta_{hk} = 0.025$ are similar to those for $\Delta_{hk} = 0.05$ and they have not been reported). The outer integral has been numerically evaluated with 8-nodes classical Gauss-Legendre formula, recalling that for $\Delta_{hk} = 0.15$ the outer integration interval does not need a subdivision while for $\Delta_{hk} = 0.05$ the outer interval has been divided in two subintervals, and taking into account the numerical analysis presented in Table 1. To conclude, when the boundary of the 2D region $r < \Delta_{hk}$, where the Heaviside function is not trivial, is contained in the rectangle $[0, 2l_i] \times [0, 2l_j]$, we will have to treat hypersingularities, on coincident and consecutive elements, together with the mild singularities related to the presence of the function $\sqrt{\Delta_{hk}^2 - r^2}$.

Case I: $\log r$ *kernel*

Coincident boundary elements

We have to numerically evaluate

$$\int_a^b \tilde{w}_m^{(d_i)}(s) \int_{M_s}^{m_s} \log|z - s| \, \tilde{w}_n^{(d_i)}(z) \, dz \, ds \,. \tag{56}$$

Outer integral: since the inner integral, as a function of the variable s, is analytic everywhere except at $s = a,\ b$, where it has mild singularities, we compute the outer integral by the regularization procedure (45);

Inner integral: is evaluated by the corresponding $(d_i + 1)$-point product rule (50) for logarithmic kernel.

Table 2 reports the relative errors in the numerical evaluation of integral (32) with $2l_i = 0.1$, $d_i = 0$ (constant functions), $\Delta t = 0.025, 0.05, 0.15$ and varying parameters p and q of the regularization procedure (45) for the outer integration; the inner integration has been performed with 1 node.

Table 2. *Relative errors in the numerical evaluation of integral* (32) *for different values of parameters* p, q *in the outer integration.*

Δt	n. nodes	$p = q = 1$	$p = q = 2$	$p = q = 3$
0.025	4	$3.8963 \cdot 10^{-5}$	$2.5899 \cdot 10^{-5}$	$4.1954 \cdot 10^{-4}$
	8	$2.9342 \cdot 10^{-6}$	$8.8273 \cdot 10^{-8}$	$2.8553 \cdot 10^{-8}$
	16	$2.0422 \cdot 10^{-7}$	$--$	$--$
0.05	4	$1.0397 \cdot 10^{-4}$	$6.9113 \cdot 10^{-5}$	$1.1195 \cdot 10^{-6}$
	8	$7.8300 \cdot 10^{-6}$	$2.3555 \cdot 10^{-7}$	$7.6194 \cdot 10^{-8}$
	16	$5.4497 \cdot 10^{-7}$	$--$	$--$
0.15	4	$3.4143 \cdot 10^{-4}$	$2.2695 \cdot 10^{-4}$	$3.6764 \cdot 10^{-3}$
	8	$2.5712 \cdot 10^{-6}$	$7.7354 \cdot 10^{-7}$	$2.5021 \cdot 10^{-7}$
	16	$1.7896 \cdot 10^{-6}$	$--$	$--$
	32	$1.1852 \cdot 10^{-7}$		

Consecutive aligned boundary elements ($e_j \equiv e_{i+1}$)

We have to numerically evaluate

$$\int_a^b \tilde{w}_m^{(d_i)}(s) \int_0^{m_s} \log|z + s| \, \tilde{w}_n^{(d_j)}(z) \, dz \, ds \,. \tag{57}$$

• if $a = 0$

Outer integral: regularization procedure (45);
Inner integral: $(d_j + 1)$-point product rule (50) for logarithmic kernel;

• otherwise

Outer integral: Gauss-Legendre rule;
Inner integral: Gauss-Legendre rule.

In Table 3 we present the relative errors in the numerical evaluation of the integral (35) with $2l_i = 0.1$, $2l_j = 0.15$, polynomial functions of degree $d_i = d_j = 0$, $\Delta t = 0.05, 0.12, 0.20, 0.26$ and varying parameters p and q of the regularization procedure (45) for the outer integration; the inner integration has been performed with 1 node. Note that for $\Delta t = 0.2$ we break in two subintervals the outer integration interval.

Table 3. *Relative errors in the numerical evaluation of integral* (35) *for different values of parameters* p, q *in the outer integration.*

Δt	n. nodes	$p = q = 1$	$p = q = 2$	$p = q = 3$
0.05	4	$3.7141 \cdot 10^{-4}$	$2.4688 \cdot 10^{-4}$	$3.9992 \cdot 10^{-3}$
	8	$2.7969 \cdot 10^{-5}$	$8.4144 \cdot 10^{-7}$	$2.7217 \cdot 10^{-7}$
	16	$1.9467 \cdot 10^{-6}$	$3.5509 \cdot 10^{-9}$	$--$
	32	$1.2892 \cdot 10^{-7}$	$--$	
0.12	4	$3.5223 \cdot 10^{-4}$	$2.3413 \cdot 10^{-4}$	$3.7927 \cdot 10^{-3}$
	8	$2.6525 \cdot 10^{-5}$	$7.9799 \cdot 10^{-7}$	$2.5812 \cdot 10^{-7}$
	16	$1.8461 \cdot 10^{-6}$	$3.3676 \cdot 10^{-9}$	$--$
	32	$1.2226 \cdot 10^{-7}$	$--$	
0.20	4	$5.2266 \cdot 10^{-5}$	$2.9853 \cdot 10^{-5}$	$7.2134 \cdot 10^{-4}$
	8	$3.9358 \cdot 10^{-6}$	$1.1828 \cdot 10^{-7}$	$6.4862 \cdot 10^{-8}$
	16	$2.7393 \cdot 10^{-7}$	$--$	$--$
0.26	4	$1.9692 \cdot 10^{-4}$	$1.6627 \cdot 10^{-4}$	$1.3194 \cdot 10^{-3}$
	8	$1.4829 \cdot 10^{-5}$	$4.4629 \cdot 10^{-7}$	$8.8858 \cdot 10^{-8}$
	16	$1.0321 \cdot 10^{-6}$	$--$	$--$
	32	$6.8355 \cdot 10^{-8}$		

Consecutive not aligned boundary elements ($e_j \equiv e_{i+1}$)

Having set $a_s = -s\cos\omega$ and $b_s = s\sin\omega$, we have to numerically evaluate

$$\frac{1}{2}\int_a^b \tilde{w}_m^{(d_i)}(s) \int_{M_s}^{m_s} \log\left[(z-a_s)^2 + b_s^2\right] \tilde{w}_n^{(d_j)}(z)\, dz\, ds\,. \tag{58}$$

• if $a = 0$ and $M_s = 0$

Outer integral: regularization procedure (45);
Inner integral: $(d_j + 1)$-point product rule (50) for logarithmic kernel;

• otherwise

Outer integral: Gauss-Legendre rule;
Inner integral: Gauss-Legendre rule.

Table 4. *Relative errors in the numerical evaluation of integral* (58) *with different values of the angle* ω *and varying parameters* p *and* q *in the outer integration.*

ω	Δt	n. nodes	$p=q=1$	$p=q=2$	$p=q=3$
$\pi/4$	0.08	4	$7.9010\cdot10^{-5}$	$6.1641\cdot10^{-5}$	$7.4587\cdot10^{-4}$
		8	$5.9409\cdot10^{-6}$	$1.6886\cdot10^{-7}$	$8.3889\cdot10^{-8}$
		16	$4.0423\cdot10^{-7}$	$--$	$--$
$\pi/2$	0.05	4	$1.7935\cdot10^{-3}$	$2.5718\cdot10^{-5}$	$2.0949\cdot10^{-3}$
		8	$2.6073\cdot10^{-4}$	$1.0739\cdot10^{-9}$	$3.4341\cdot10^{-7}$
		16	$3.5439\cdot10^{-5}$	$--$	$--$
		32	$4.6304\cdot10^{-6}$		
		64	$5.9213\cdot10^{-7}$		
$\pi/2$	0.12	4	$5.2240\cdot10^{-8}$	$3.0974\cdot10^{-5}$	$2.9088\cdot10^{-4}$
		8	$--$	$1.2340\cdot10^{-10}$	$8.4666\cdot10^{-8}$
$5\pi/8$	0.095	4	$4.3607\cdot10^{-6}$	$3.9587\cdot10^{-5}$	$4.8712\cdot10^{-4}$
		8	$1.8580\cdot10^{-7}$	$3.1168\cdot10^{-8}$	$2.4127\cdot10^{-7}$

In Table 4 we present the relative errors in the numerical evaluation of integral (58) with $2l_i = 2l_j = 0.1$, polynomial functions of degree $d_i = d_j = 0$, different values of time step Δt, angle $\omega = \pi/4,\ \pi/2,\ 5\pi/8$ and varying the parameters p, q of the regularization procedure (45) for the outer integration.

Case II: $\dfrac{\mathbf{r}\cdot\mathbf{n}_\xi}{r^2}\ \sqrt{\Delta_{hk}^2 - r^2}$ *kernel*

Note that, due to the presence of the scalar product $\mathbf{r}\cdot\mathbf{n}_\xi$, the coincident and consecutive aligned elements cases have not to be considered.

Consecutive not aligned boundary elements ($e_j \equiv e_{i+1}$)

Having set $a_s = -s\cos\omega$ and $b_s = s\sin\omega$, we have to numerically evaluate

$$\int_a^b \tilde{w}_m^{(d_i)}(s) \int_{M_s}^{m_s} \frac{-b_s}{(z-a_s)^2 + b_s^2}\ \sqrt{\Delta_{hk}^2 - ((z-a_s)^2 + b_s^2)}\ \tilde{w}_n^{(d_j)}(z)\,dz\,ds\,. \tag{59}$$

Two subcases arise:

i) the boundary of the 2D region $r < \Delta_{hk}$ is not contained in the rectangle $[a,b]\times[M_s,m_s]$, i.e. $M_s = 0, m_s = 2l_j$

• if $a = 0$

Outer integral: regularization procedure (45);
Inner integral: product rule (50) for $[(z-a_s)^2+b_s^2]^{-1}$ kernel;

• otherwise

Outer integral: Gauss-Legendre rule;
Inner integral: Gauss-Legendre rule.

ii) the boundary of the 2D region $r<\Delta_{hk}$ is contained in the rectangle $[a,b]\times[M_s,m_s]$

• if $a=0$ and $M_s=0$ we rewrite the double integral (59) in the form:

$$\mathcal{I} = -\int_0^b b_s\,\tilde{w}_m^{(d_i)}(s)\int_0^{m_s}\frac{\sqrt{\Delta_{hk}^2-((z-a_s)^2+b_s^2)}\;\tilde{w}_n^{(d_j)}(z)-\Delta_{hk}\tilde{w}_n^{(d_j)}(0)-\Delta_{hk}\tilde{w}_n'^{(d_j)}(0)\,z}{(z-a_s)^2+b_s^2}\,dzds$$

$$-\Delta_{hk}\,\tilde{w}_n^{(d_j)}(0)\int_0^b b_s\,\tilde{w}_m^{(d_i)}(s)\int_0^{m_s}\frac{1}{(z-a_s)^2+b_s^2}\,dz\,ds$$

$$-\Delta_{hk}\,\tilde{w}_n'^{(d_j)}(0)\int_0^b b_s\,\tilde{w}_m^{(d_i)}(s)\int_0^{m_s}\frac{z}{(z-a_s)^2+b_s^2}\,dz\,ds =: \mathcal{I}_1+\mathcal{I}_2+\mathcal{I}_3\,.$$

In particular, to evaluate $\mathcal{I}_1$ we use:

Outer integral: Gauss-Legendre rule;
Inner integral: regularization procedure (45), because of the square root mild singularity.

For $\mathcal{I}_2$, after a simple analytical inner integration we have:

$$\mathcal{I}_2 = -\Delta_{hk}\,\tilde{w}_n^{(d_j)}(0)\int_0^{2l_i}\tilde{w}_m^{(d_i)}(s)\Big[\arctan\Big(\frac{m_s-a_s}{b_s}\Big)+\arctan\Big(\frac{a_s}{b_s}\Big)\Big]\,ds$$

and we use a Gauss-Legendre rule.
For $\mathcal{I}_3$, after an analytical inner integration we have:

$$\mathcal{I}_3 = -\Delta_{hk}\,\tilde{w}_n'^{(d_j)}(0)\int_0^{2l_i}\tilde{w}_m^{(d_i)}(s)\,a_s\Big[\arctan\Big(\frac{m_s-a_s}{b_s}\Big)+\arctan\Big(\frac{a_s}{b_s}\Big)\Big]\,ds$$

$$-\Delta_{hk}\,\tilde{w}_n'^{(d_j)}(0)\int_0^{2l_i}\tilde{w}_m^{(d_i)}(s)\frac{b_s}{2}\,\Big[\log\left((m_s-a_s)^2+b_s^2\right)-\log\left(a_s^2+b_s^2\right)\Big]\,ds$$

$$=: \mathcal{I}_3^1+\mathcal{I}_3^2.$$

For the numerical evaluation of $\mathcal{I}_3^1$ we use a Gauss-Legendre formula, while for $\mathcal{I}_3^2$ we use regularization procedure (45), because of the logarithmic mild singularities.

• otherwise

the singularity point is not contained in the domain of integration, hence for the numerical evaluation of (59) we proceed as follows:

Outer integral: Gauss-Legendre rule;
Inner integral: regularization procedure (45), because of the square root mild singularity.

Table 5. *Relative errors w.r.t. the integral value $\mathcal{I}_1$ evaluated with Mathematica.*

n. nodes (n)	n. nodes (m)	$p=1,\ q=1$	$p=1,\ q=2$	$p=1,\ q=3$
4	4	$7.9857 \cdot 10^{-3}$	$9.5113 \cdot 10^{-3}$	$9.3910 \cdot 10^{-3}$
	8	$9.1143 \cdot 10^{-3}$	$9.3177 \cdot 10^{-3}$	$9.3178 \cdot 10^{-3}$
	16	$9.2897 \cdot 10^{-3}$	$9.3177 \cdot 10^{-3}$	$9.3177 \cdot 10^{-3}$
8	4	$4.3570 \cdot 10^{-5}$	$1.5686 \cdot 10^{-3}$	$1.4399 \cdot 10^{-3}$
	8	$1.1713 \cdot 10^{-3}$	$1.3747 \cdot 10^{-3}$	$1.3748 \cdot 10^{-3}$
	16	$1.3467 \cdot 10^{-3}$	$1.3745 \cdot 10^{-3}$	$1.3747 \cdot 10^{-3}$
16	4	$1.1435 \cdot 10^{-3}$	$3.8142 \cdot 10^{-4}$	$2.5237 \cdot 10^{-4}$
	8	$1.5780 \cdot 10^{-5}$	$1.8757 \cdot 10^{-4}$	$1.8762 \cdot 10^{-4}$
	16	$1.5953 \cdot 10^{-4}$	$1.8757 \cdot 10^{-4}$	$1.8757 \cdot 10^{-4}$
32	4	$1.3066 \cdot 10^{-3}$	$2.1839 \cdot 10^{-4}$	$8.9323 \cdot 10^{-5}$
	8	$1.7881 \cdot 10^{-4}$	$2.4538 \cdot 10^{-5}$	$2.4592 \cdot 10^{-5}$
	16	$3.4971 \cdot 10^{-6}$	$2.4533 \cdot 10^{-5}$	$2.4534 \cdot 10^{-5}$
	32	$2.0857 \cdot 10^{-6}$	$2.4530 \cdot 10^{-5}$	$2.4533 \cdot 10^{-5}$
64	4	$1.3066 \cdot 10^{-3}$	$1.9699 \cdot 10^{-4}$	$6.7929 \cdot 10^{-5}$
	8	$2.0021 \cdot 10^{-4}$	$3.1456 \cdot 10^{-6}$	$3.1988 \cdot 10^{-6}$
	16	$2.4890 \cdot 10^{-5}$	$3.1401 \cdot 10^{-6}$	$3.1409 \cdot 10^{-6}$
	32	$5.3597 \cdot 10^{-7}$	$3.1399 \cdot 10^{-6}$	$3.1406 \cdot 10^{-6}$

Tables 5 and 6 report the relative errors obtained in the numerical evaluation of integrals $\mathcal{I}_1$, $\mathcal{I}_2$, $\mathcal{I}_3$ with $2l_i = 2l_j = 0.1$, $\Delta_{hk} = 0.05$, $\omega = \pi/2$ and interpolation polynomials with local degree $d_i = 0$, $d_j = 1$, respectively. For $\mathcal{I}_1$ the integration has been performed with $n \times m$ nodes Gauss-Legendre rule and varying the parameters p, q of the regularization procedure (45) for the outer integral.

Table 6. *Relative error w.r.t. the integral value $\mathcal{I}_2$ and the integral value $\mathcal{I}_3$ evaluated with Mathematica. The symbol $--$ means that the single precision accuracy has been achieved.*

n. nodes	$\mathcal{I}_2$	$\mathcal{I}_3$		
		$p=q=1$	$p=q=2$	$p=q=3$
4	$1.6361 \cdot 10^{-3}$	$2.5968 \cdot 10^{-3}$	$1.7261 \cdot 10^{-3}$	$2.7960 \cdot 10^{-2}$
8	$2.3865 \cdot 10^{-4}$	$1.9568 \cdot 10^{-4}$	$6.0198 \cdot 10^{-6}$	$2.0397 \cdot 10^{-6}$
16	$3.2469 \cdot 10^{-5}$	$1.3747 \cdot 10^{-5}$	$1.6171 \cdot 10^{-7}$	$1.3719 \cdot 10^{-7}$
32	$4.2433 \cdot 10^{-6}$	$1.0382 \cdot 10^{-6}$	$--$	$--$
64	$5.4266 \cdot 10^{-7}$	$1.9494 \cdot 10^{-7}$		

Case III: $\left[\dfrac{(\mathbf{r}\cdot\mathbf{n}_\mathbf{x})(\mathbf{r}\cdot\mathbf{n}_\xi)}{r^2} - \dfrac{\mathbf{n}_\mathbf{x}\cdot\mathbf{n}_\xi}{2}\right]\dfrac{\sqrt{\Delta_{hk}^2 - r^2}}{r^2}$ *kernel*

Coincident boundary elements ($e_i \equiv e_j$)

Note that in this configuration $\mathbf{r}\cdot\mathbf{n}_\mathbf{x} = \mathbf{r}\cdot\mathbf{n}_\xi = 0$, $\mathbf{n}_\mathbf{x}\cdot\mathbf{n}_\xi = 1$ and we have to numerically evaluate

$$\mathcal{I} = -\frac{1}{2}\int_a^b \tilde{w}_i^{(d_i)}(s) \int_{M_s}^{m_s} \frac{\sqrt{\Delta_{hk}^2 - r^2}}{|z-s|^2}\, \tilde{w}_j^{(d_j)}(z)\, dz\, ds\,. \tag{60}$$

Two subcases arise:

i) the boundary of the 2D region $r < \Delta_{hk}$ is not contained in the rectangle $[a,b]\times[M_s, m_s]$, i.e. $M_s = 0$, $m_s = 2l_i$.
We rewrite double integral (60) as follows:

$$\mathcal{I} = -\int_a^b \tilde{w}_m^{(d_i)}(s) \int_0^{2l_i} \frac{1}{|z-s|}\frac{\sqrt{\Delta_{hk}^2 - |z-s|^2}\,\tilde{w}_n^{(d_j)}(z) - \Delta_{hk}\,\tilde{w}_n^{(d_j)}(s)}{2\,|z-s|}\, dz\, ds$$
$$-\frac{\Delta_{hk}}{2}\int_a^b \tilde{w}_m^{(d_i)}(s)\,\tilde{w}_n^{(d_j)}(s) \int_0^{2l_i} \frac{1}{|z-s|^2}\, dz\, ds =: \mathcal{I}_1 + \mathcal{I}_2\,.$$

For the numerical evaluation of $\mathcal{I}_1$ we use:

Outer integral: regularization procedure (45);
Inner integral: product rule (50) for $|z-s|^{-1}$ kernel, to treat the strong singularity (here we recall that the square root mild singularity is non present).

For $\mathcal{I}_2$, after an analytical inner integration we have:

$$\mathcal{I}_2 = -\frac{\Delta_{hk}}{2}\int_a^b \tilde{w}_m^{(d_i)}(s)\,\tilde{w}_n^{(d_j)}(s)\left[\frac{1}{s-2l_i}-\frac{1}{s}\right]ds =: \mathcal{I}_2^1 + \mathcal{I}_2^2\,.$$

$\mathcal{I}_2^1$ and $\mathcal{I}_2^2$ can be evaluated with the $\lceil (d_i+d_j)/2 \rceil$ points HFP quadrature rule (53) if respectively $b = 2l_i$, $a = 0$, otherwise with the Gauss-Legendre formula.

ii) the boundary of the 2D region $r < \Delta_{hk}$ is contained in the rectangle $[a,b]\times[M_s, m_s]$.
In this case, we have to rewrite the double integral (60) as:

$$\mathcal{I} = -\int_a^b \tilde{w}_m^{(d_i)}(s)\int_{M_s}^{m_s}\frac{\sqrt{\Delta_{hk}^2 - |z-s|^2}\,\tilde{w}_n^{(d_j)}(z) - \Delta_{hk}\tilde{w}_n^{(d_j)}(s) - \Delta_{hk}\tilde{w}_n^{\prime(d_j)}(s)(z-s)}{2\,|z-s|^2}\,dz\,ds$$

$$-\frac{\Delta_{hk}}{2}\int_a^b \tilde{w}_m^{(d_i)}(s)\,\tilde{w}_n^{(d_j)}(s)\int_{M_s}^{m_s}\frac{1}{|z-s|^2}\,dz\,ds$$

$$-\frac{\Delta_{hk}}{2}\int_a^b \tilde{w}_m^{(d_i)}(s)\,\tilde{w}_n^{\prime(d_j)}(s)\int_{M_s}^{m_s}\frac{1}{|z-s|}\,dz\,ds =: \mathcal{I}_1 + \mathcal{I}_2 + \mathcal{I}_3\,.$$

For the numerical evaluation of $\mathcal{I}_1$ we use:

Outer integral: Gauss-Legendre rule;
Inner integral: regularization procedure (45), to treat the square root mild singularity alone (the hypersingularity has been completely removed).

Table 7 shows the relative errors in the evaluating the integral $\mathcal{I}_1$ referred to the discretization parameters $2l_i = 0.1$, $\Delta_{hk} = 0.05$, $d_i = d_j = 1$ and varying the

Table 7. *Relative errors w.r.t. the integral value $\mathcal{I}_1$ evaluated with Mathematica.*

n. of nodes	$p = q = 1$	$p = q = 2$	$p = q = 3$
4	$1.4476 \cdot 10^{-3}$	$1.9274 \cdot 10^{-4}$	$8.0499 \cdot 10^{-4}$
8	$2.0551 \cdot 10^{-4}$	$2.5891 \cdot 10^{-6}$	$1.3695 \cdot 10^{-6}$
16	$2.7796 \cdot 10^{-5}$	$1.2145 \cdot 10^{-7}$	$1.2213 \cdot 10^{-7}$
32	$3.6601 \cdot 10^{-6}$	$--$	$--$

parameters p and q for the inner integration. The outer integration has been performed with 16-nodes Gauss-Legendre rule. For $\mathcal{I}_2$, after an analytical inner integration we have:

$$\mathcal{I}_2 = -\frac{\Delta_{hk}}{2}\int_a^b \tilde{w}_m^{(d_i)}(s)\,\tilde{w}_n^{(d_j)}(s)\left[\frac{1}{s-m_s}-\frac{1}{s-M_s}\right]ds =: \mathcal{I}_2^1 + \mathcal{I}_2^2\,.$$

$\mathcal{I}_2^1$ and $\mathcal{I}_2^2$ can be evaluated with the $\lceil (d_i+d_j)/2 \rceil$ points HFP quadrature rule (53) if, respectively, $m_s = 2l_i$ and $b = 2l_i$, $M_s = 0$ and $a = 0$, otherwise with the Gauss-Legendre formula. For $\mathcal{I}_3$, after an analytical inner integration we have:

$$\mathcal{I}_3 = -\frac{\Delta_{hk}}{2}\int_a^b \tilde{w}_m^{(d_i)}(s)\,\tilde{w}_n'^{(d_j)}(s)[\log|m_s-s| - \log|M_s-s|]\,ds =: \mathcal{I}_3^1 + \mathcal{I}_3^2\,.$$

If $m_s = 2l_i$ and $b = 2l_i$, $\mathcal{I}_3^1$ can be evaluated with the regularization procedure (45), because of the logarithmic singularities, otherwise with the Gauss-Legendre formula. Analogously, if $M_s = 0$ and $a = 0$ for the integral $\mathcal{I}_3^2$.

`Consecutive aligned boundary elements` ($e_j \equiv e_{i+1}$)

Note that in this configuration $\mathbf{r}\cdot\mathbf{n_x} = \mathbf{r}\cdot\mathbf{n_\xi} = 0$, $\mathbf{n_x}\cdot\mathbf{n_\xi} = 1$ and the singularity point is only in $\bar{e}_i \cap \bar{e}_j$,

$$\mathcal{I} = -\frac{1}{2}\int_a^b \tilde{w}_m^{(d_i)}(s)\int_0^{m_s}\frac{\sqrt{\Delta_{hk}^2-(z+s)^2}}{(z+s)^2}\,\tilde{w}_n^{(d_j)}(z)\,dz\,ds\,. \tag{61}$$

Two subcases arise:

i) the boundary of the 2D region $r<\Delta_{hk}$ is not contained in the rectangle $[a,b]\times[0,m_s]$, i.e. $m_s = 2l_j$

• if $b = 2l_i$, we rewrite double integral (61) as follows:

$$\mathcal{I} = -\frac{1}{2}\int_0^{2l_i}\tilde{w}_m^{(d_i)}(s)\int_0^{2l_j}\frac{1}{(z+s)}\frac{\sqrt{\Delta_{hk}^2-(z+s)^2}\tilde{w}_n^{(d_j)}(z)-\Delta_{hk}\,\tilde{w}_n^{(d_j)}(0)}{(z+s)}\,dzds$$

$$-\frac{\Delta_{hk}}{2}\,\tilde{w}_n^{(d_j)}(0)\int_a^{2l_i}\tilde{w}_m^{(d_i)}(s)\int_0^{m_s}\frac{1}{(z+s)^2}\,dz\,ds =: \mathcal{I}_1 + \mathcal{I}_2\,.$$

For the numerical evaluation of $\mathcal{I}_1$ we use:

Outer integral: regularization procedure (45);
Inner integral: product rule (50) for $(z+s)^{-1}$ kernel.

For $\mathcal{I}_2$, after an analytical inner integration we have:

$$\mathcal{I}_2 = -\frac{\Delta_{hk}}{2}\,\tilde{w}_n^{(d_j)}(0)\int_a^{2l_i}\tilde{w}_m^{(d_i)}(s)\left[\frac{1}{s}-\frac{1}{s+2l_j}\right]ds =: \mathcal{I}_2^1+\mathcal{I}_2^2$$

$\mathcal{I}_2^1$ can be evaluated with the $\lceil d_i/2\rceil$ points HFP quadrature rule (53) and $\mathcal{I}_2^2$ with the Gauss-Legendre rule.

• Otherwise, i.e when the singularity point is not contained in the integration domain, for the numerical evaluation of (61) we can proceed as follows:
Outer integral: Gauss-Legendre rule;
Inner integral: Gauss-Legendre rule.

ii) the boundary of the 2D region $r<\Delta_{hk}$ is contained in the rectangle $[a,b]\times[0,m_s]$

• if $b=2l_i$, we have to rewrite the double integral (61) as:

$$\begin{aligned}\mathcal{I} = &-\int_a^{2l_i}\tilde{w}_m^{(d_i)}(s)\int_0^{m_s}\frac{\sqrt{\Delta_{hk}^2-(z+s)^2}\,\tilde{w}_n^{(d_j)}(z)-\Delta_{hk}\tilde{w}_n^{(d_j)}(0)-\Delta_{hk}\tilde{w}_n'^{(d_j)}(0)\,z}{2(z+s)^2}\,dzds\\ &-\frac{\Delta_{hk}}{2}\,\tilde{w}_n^{(d_j)}(0)\int_a^{2l_i}\tilde{w}_m^{(d_i)}(s)\int_0^{m_s}\frac{1}{(z+s)^2}\,dzds\\ &-\frac{\Delta_{hk}}{2}\,\tilde{w}_n'^{(d_j)}(0)\int_a^{2l_i}\tilde{w}_m^{(d_i)}(s)\int_0^{m_s}\frac{z}{(z+s)^2}\,dzds =: \mathcal{I}_1+\mathcal{I}_2+\mathcal{I}_3\,.\end{aligned}$$

For the numerical evaluation of $\mathcal{I}_1$ we use:

Outer integral: Gauss-Legendre rule;
Inner integral: regularization procedure (45), because of the square root mild singularity.

For $\mathcal{I}_2$, after an analytical inner integration we have:

$$\mathcal{I}_2 = -\frac{\Delta_{hk}}{2}\,\tilde{w}_n^{(d_j)}(0)\int_a^{2l_i}\tilde{w}_m^{(d_i)}(s)\left[\frac{1}{s}-\frac{1}{s+m_s}\right]ds =: \mathcal{I}_2^1+\mathcal{I}_2^2$$

$\mathcal{I}_2^1$ can be evaluated with the $\lceil d_i/2\rceil$ points HFP quadrature rule (53) and $\mathcal{I}_2^2$ with the Gauss-Legendre rule.

For $\mathcal{I}_3$, after an analytical inner integration we have:

$$\mathcal{I}_3 = -\frac{\Delta_{hk}}{2}\tilde{w}_n^{\prime(d_j)}(0)\int_a^{2l_i}\tilde{w}_m^{(d_i)}(s)\left[\frac{(m_s-a_s)\log(m_s-a_s)-m_s}{m_s-a_s}-\log(-a_s)\right]ds$$
$$=: \mathcal{I}_3^1 + \mathcal{I}_3^2.$$

For the numerical evaluation of $\mathcal{I}_3^1$ we use the Gauss-Legendre formula, while for $\mathcal{I}_3^2$ we can use the regularization procedure (45), because of the logarithmic mild singularity.

• Otherwise, i.e. when the singularity point is not contained in the domain of integration, for the numerical evaluation of (61) we can proceed as follows:

Outer integral: Gauss-Legendre rule;
Inner integral: regularization procedure (45), because of the square root mild singularity.

Consecutive not aligned boundary elements ($e_j \equiv e_{i+1}$)

Having set $a_s = -s\cos\omega$ and $b_s = s\sin\omega$, we have to evaluate

$$\begin{aligned}\mathcal{I} = &-\int_a^b \tilde{w}_m^{(d_i)}(s)\int_{M_s}^{m_s}\frac{\cos\omega}{2}\frac{\sqrt{\Delta_{hk}^2-((z-a_s)^2+b_s^2)}}{(z-a_s)^2+b_s^2}\tilde{w}_n^{(d_j)}(z)\,dzds\\ &-\int_a^b \tilde{w}_m^{(d_i)}(s)\int_{M_s}^{m_s}(b_s z\sin\omega)\frac{\sqrt{\Delta_{hk}^2-((z-a_s)^2+b_s^2)}}{((z-a_s)^2+b_s^2)^2}\tilde{w}_n^{(d_j)}(z)\,dzds\\ =:&\,\mathcal{I}_1+\mathcal{I}_2.\end{aligned} \tag{62}$$

Here, we will treat only the double integral $\mathcal{I}_2$, the integral $\mathcal{I}_1$ being evaluated in a similar way.
For the evaluation of $\mathcal{I}_2$ the standard two subcases arise:

i) the boundary of the 2D region $r<\Delta_{hk}$ is not contained in the rectangle $[a,b]\times[M_s,m_s]$, i.e. $M_s=0$, $m_s=2l_j$.

• If $b=2l_i$, we rewrite double integral $\mathcal{I}_2$ as

$$\mathcal{I}_2 = -\int_a^{2l_i}\tilde{w}_m^{(d_i)}(s)\int_0^{2l_j}\frac{zb_s\sin\omega}{((z-a_s)^2+b_s^2)^2}$$
$$\left[\tilde{w}_n^{(d_j)}(z)\sqrt{\Delta_{hk}^2-((z-a_s)^2+b_s^2)}-\Delta_{hk}\tilde{w}_n^{(d_j)}(0)-\Delta_{hk}\tilde{w}_n^{\prime(d_j)}(0)z\right]dzds$$

$$- \Delta_{hk}\, \tilde{w}_n^{(d_j)}(0) \int_a^{2l_i} \tilde{w}_m^{(d_i)}(s) \int_0^{2l_j} \frac{z b_s \sin\omega}{((z-a_s)^2 + b_s^2)^2}\, dz\, ds$$

$$- \Delta_{hk} \tilde{w}_n'^{(d_j)}(0) \int_a^{2l_i} \tilde{w}_m^{(d_i)}(s) \int_0^{2l_j} \frac{z^2 b_s \sin\omega}{((z-a_s)^2 + b_s^2)^2}\, dz\, ds =: \mathcal{I}_2^1 + \mathcal{I}_2^2 + \mathcal{I}_2^3 .$$

For the numerical evaluation of $\mathcal{I}_2^1$ we use:

Outer integral: regularization procedure (45);
Inner integral: product rule (50) for $z\,[(z-a_s)^2 + b_s^2]^{-1}$ kernel.

For $\mathcal{I}_2^2$, after an analytical inner integration we have:

$$\mathcal{I}_2^2 = -\Delta_{hk} \sin\omega\, \tilde{w}_n^{(d_j)}(0) \int_a^{2l_i} \tilde{w}_m^{(d_i)}(s)\, [f(2l_j, s) - f(0, s)]\, ds ,$$

with

$$f(z,s) = \frac{1}{2\, b_s} \left[\frac{z a_s - (a_s^2 + b_s^2)}{((z-a_s)^2 + b_s^2)} - \operatorname{atan}(\omega) \operatorname{atan}\left(\frac{z-a_s}{b_s} \right) \right], \tag{63}$$

that can be evaluated with the HFP quadrature rule (53).
For $\mathcal{I}_2^3$, after an analytical inner integration we have:

$$\mathcal{I}_2^3 = -\Delta_{hk} \sin\omega\, \tilde{w}_n'^{(d_j)}(0) \int_a^{2l_i} \tilde{w}_m^{(d_i)}(s) [f(2l_j, s) - f(0, s)] ds ,$$

with

$$f(z,s) = \frac{b_s(-a_s + z(\cos^2\omega - \sin^2\omega))}{2\sin^2\omega\, ((z-a_s)^2 + b_s^2)} - \frac{1}{2} \operatorname{atan}\left(\frac{z-a_s}{b_s} \right), \tag{64}$$

that can be evaluated with the Gauss-Legendre formula.

• Otherwise, i.e when the singularity point is not contained in the integration domain, for the numerical evaluation of $\mathcal{I}_2$ we can proceed as follows:

Outer integral: Gauss-Legendre rule;
Inner integral: Gauss-Legendre rule.

ii) the boundary of the 2D region $r < \Delta_{hk}$ is contained in the rectangle $[a, b] \times [M_s, m_s]$.

• If $b = 2l_i$ and $M_s = 0$, we have to rewrite the double integral $\mathcal{I}_2$ in the form

$$
\begin{aligned}
(65)\qquad \mathcal{I}_2 = &-\int_a^{2l_i} \tilde{w}_m^{(d_i)}(s) \int_0^{m_s} \frac{b_s z \sin\omega}{((z-a_s)^2+b_s^2)^2} \left[\tilde{w}_n^{(d_j)}(z)\sqrt{\Delta_{hk}^2-((z-a_s)^2+b_s^2)} \right. \\
&\left. - \Delta_{hk}\tilde{w}_n^{(d_j)}(0) - \Delta_{hk}\tilde{w}_n'^{(d_j)}(0)z - \frac{z^2}{2}\left(\tilde{w}_n''^{(d_j)}(0)\Delta_{hk} - \frac{\tilde{w}_n^{(d_j)}(0)}{\Delta_{hk}} \right) \right] dzds \\
&+ \Delta_{hk}\,\tilde{w}_n^{(d_j)}(0) \int_a^{2l_i} -\tilde{w}_n^{(d_i)}(s) \int_0^{m_s} \frac{z b_s \sin\omega}{((z-a_s)^2+b_s^2)^2}\, dzds \\
&- \Delta_{hk}\tilde{w}_n'^{(d_j)}(0) \int_a^{2l_i} \tilde{w}_m^{(d_i)}(s) \int_0^{m_s} \frac{z^2 b_s \sin\omega}{((z-a_s)^2+b_s^2)^2}\, dzds \\
&- \Delta_{hk}\left[\tilde{w}_n''^{(d_j)}(0)\Delta_{hk} - \frac{\tilde{w}_n^{(d_j)}(0)}{\Delta_{hk}} \right] \int_a^{2l_i} \tilde{w}_m^{(d_i)}(s) \int_0^{m_s} \frac{z^3 b_s \sin\omega}{((z-a_s)^2+b_s^2)^2}\, dzds \\
&=: \mathcal{I}_2^1 + \mathcal{I}_2^2 + \mathcal{I}_2^3 + \mathcal{I}_2^4 .
\end{aligned}
$$

For the numerical evaluation of $\mathcal{I}_2^1$ we use:

Outer integral: Gauss-Legendre formula;
Inner integral: regularization procedure (45), because of the square root mild singularity.

For $\mathcal{I}_2^2$, after an analytical inner integration we have:

$$
\mathcal{I}_2^2 = -\Delta_{hk}\sin\omega\,\tilde{w}_n^{(d_j)}(0) \int_a^{2l_i} \tilde{w}_m^{(d_i)}(s)\,[f(m_s,s)-f(0,s)]ds
$$

with $f(z,s)$ given in (63), that can be evaluated with the HFP quadrature rule (53).
For $\mathcal{I}_2^3$, after an analytical inner integration we have:

$$
\mathcal{I}_2^3 = -\Delta_{hk}\sin\omega\,\tilde{w}_n'^{(d_j)}(0) \int_a^{2l_i} \tilde{w}_m^{(d_i)}(s)\,[f(m_s,s)-f(0,s)]ds
$$

with $f(z)$ given in (64), that can be evaluated with the Gauss-Legendre rule.
For $\mathcal{I}_2^4$, after an analytical inner integration we have:

$$
\mathcal{I}_2^4 = -\left[\tilde{w}_n''^{(d_j)}(0)\Delta_{hk}^2 - \tilde{w}_n^{(d_j)}(0) \right] \int_a^{2l_i} \tilde{w}_m^{(d_i)}(s)\,(b_s\sin\omega)\,[f(m_s,s)-f(0,s)]ds
$$

Table 8. *Relative error w.r.t. the integral value $\mathcal{I}_2^1$ evaluated with Mathematica.*

n. of nodes	$p = q = 1$	$p = q = 2$	$p = q = 3$
8	$1.0515 \cdot 10^{-3}$	$1.8047 \cdot 10^{-3}$	$2.6107 \cdot 10^{-3}$
16	$3.9256 \cdot 10^{-5}$	$3.4677 \cdot 10^{-5}$	$1.9690 \cdot 10^{-5}$
32	$2.0713 \cdot 10^{-6}$	$2.8574 \cdot 10^{-7}$	$2.7491 \cdot 10^{-8}$

Table 9. *Relative error w.r.t. the integral values $\mathcal{I}_2^2, \mathcal{I}_2^3, \mathcal{I}_2^4$ evaluated with Mathematica.*

n. of nodes	$\mathcal{I}_2^2$	$\mathcal{I}_2^3$	$\mathcal{I}_2^4$
2	$1.2324 \cdot 10^{-15}$	$3.4275 \cdot 10^{-5}$	
4	$--$	$1.1839 \cdot 10^{-5}$	
8		$3.0919 \cdot 10^{-6}$	$4.8014 \cdot 10^{-4}$
16		$--$	$3.3186 \cdot 10^{-5}$
32			$2.1933 \cdot 10^{-6}$

with

$$f(z,s) = \frac{1}{2}\log\left((z-a_s)^2 + b_s^2\right) - \frac{(\cos^3\omega + 3\sin^2\omega\cos\,\omega)}{2\sin^3\omega}\operatorname{atan}\left(\frac{z-a_s}{b_s}\right) + \frac{a_s^4 - b_s^4 - z a_s^3 - 3 z a_s b_s^2}{2b_s^2((z-a_s)^2 + b_s^2)}$$

that can be evaluated with the Gauss-Legendre rule.

Tables 8-9 are referred to the calculation of the integral $\mathcal{I}_2$ as sum of the four integrals $\mathcal{I}_2^1, \mathcal{I}_2^2, \mathcal{I}_2^3, \mathcal{I}_2^4$ (see (66)), with $\omega = \pi/2$, $2l_i = 2l_j = 0.1$, $\Delta_{hk} = 0.05$. In particular Table 8 presents the relative errors in the numerical evaluation of $\mathcal{I}_2^1$ varying parameters p and q of the regularization procedure (45) for the inner integration; the outer integration has been performed with 16-nodes classical Gaussian rule.

• Otherwise, i.e. the singularity point is not contained in the domain of integration, for the numerical evaluation of $\mathcal{I}_2$ we can proceed as follows:

Outer integral: Gauss-Legendre rule;
Inner integral: regularization procedure (45), because of the square root mild singularity.

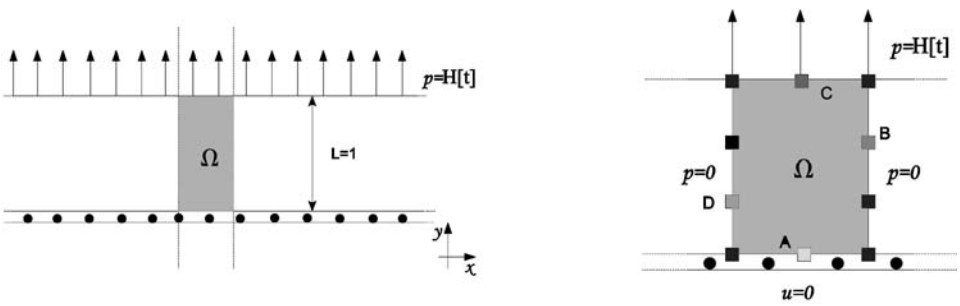

Fig. 6. Domain and mixed boundary conditions for the first test problem.

6 - Numerical results

To validate the presented discretization approach, we consider a standard benchmark (see for instance [**16**]), involving a strip Ω of unit height, unbounded in horizontal direction, fixed in the inferior part where the Dirichlet boundary datum $\bar{u} = 0$ is assigned, and subject to a uniform traction $\bar{p} = H[t]$ in its superior part, as shown in Figure 6. A finite portion of the strip is taken into account, in such a way that vertical dimension of the resulting rectangle is five times the other one. On the "cut" sides of the domain the equilibrium condition $\bar{p} = 0$ has been assigned. In order to apply energetic Galerkin BEM, we have introduced on Γ a uniform mesh with 48 elements ($\Delta x = 0.05$) and we have used, in spatial variable, constant shape functions for the approximation of p and linear shape functions for the approximation of u. The time interval of analysis $[0, 10]$ has been discretized with different time steps. In Figure 7 we show the recovered numerical solution obtained with $\Delta t = 0.035$. In particular time history of traction in the point A, $p(A, t)$ is shown on the left, together

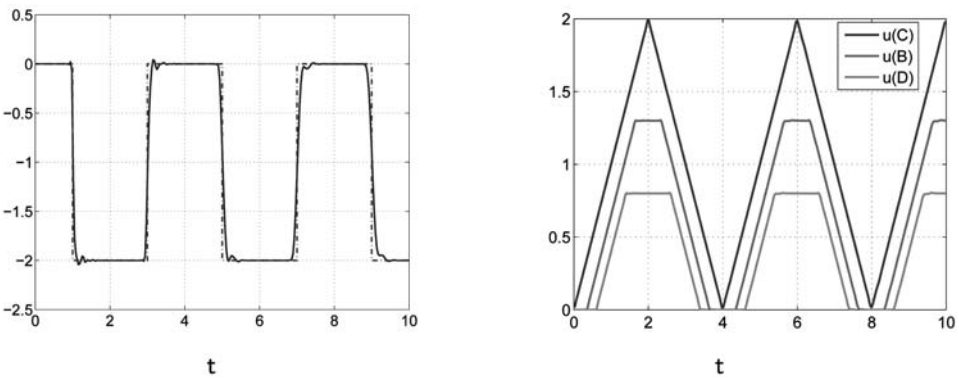

Fig. 7. Approximate solution p and u of the first test problem.

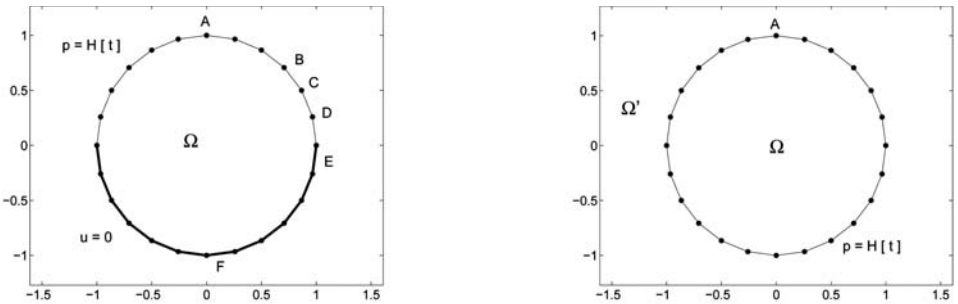

Fig. 8. Domain and boundary conditions of the second (left) and of the third (right) simulation.

with the corresponding analytical solution, while displacement in the points B, C, D, respectively $u(B,t)$, $u(C,t)$, $u(D,t)$ are shown on the right: here the three curves overlap with their respective analytical solutions. Note that the oscillations in the graph of $p(A,t)$ are due to the difficulty of approximating the jump discontinuities of the analytical solution; anyway, the obtained numerical solution is substantially better with respect to those found in literature, which present much more instability (see e.g. [**16**]).

As second simulation, we consider a unitary disk, whose upper semi-circular boundary is subject to the Neumann boundary datum $\bar{p} = H[t]$, while its lower semi-circular boundary is fixed. Domain and mixed boundary conditions are shown in Figure 8 on the left. For the discretization phase, we have approximated the boundary Γ introducing a uniform mesh with 24 straight elements and we have used, in spatial variable, constant shape functions for the approximation of p and linear shape functions for the approximation of u. The time interval of analysis $[0, 10]$ has been discretized with different time steps. In Figure 9 the approximate solution obtained with the energetic approach, fixing $\Delta t = 0.2$, is presented. In particular, on the left the time

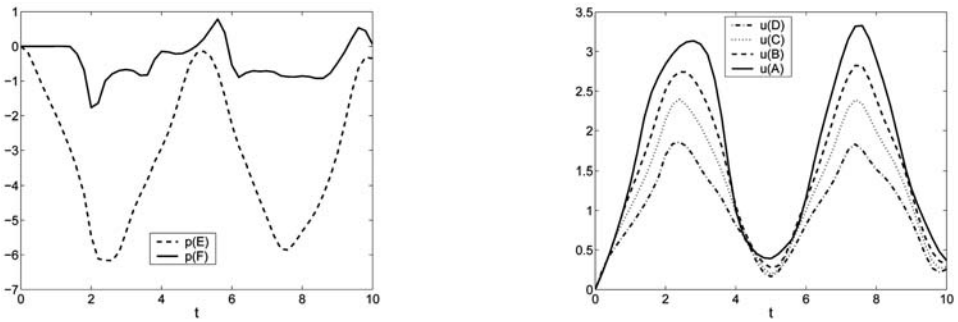

Fig. 9. Approximate solution of the second simulation.

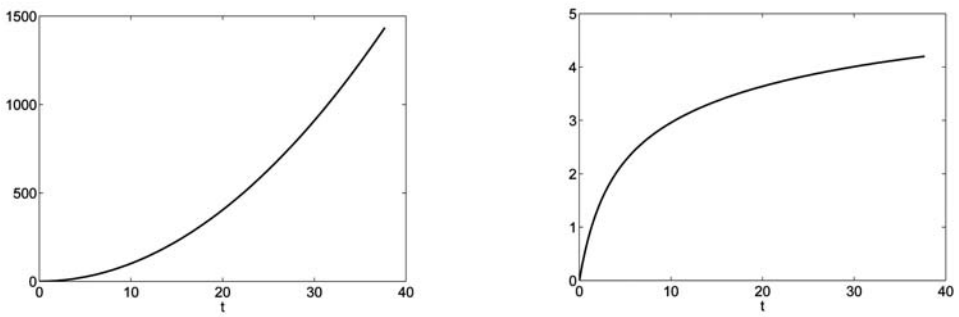

Fig. 10. Approximate solutions of the interior (left) and exterior (right) problem on the unitary circle with Neumann boundary conditions.

history $p(E,t), p(F,t)$ of p on the elements E, F is shown and one can note that while the element E near the Neumann boundary is immediately affected by the wave, the solution on the element F is trivial till the time instant $t \simeq 1.5$. On the right the time history of the solution u at nodes A, B, C, D is shown: of course, the nearer these nodes are to Γ_u, which is fixed, the lower is the value of the corresponding solution.

At last we consider the same domain of the previous simulation, subject to pure Neumann boundary conditions $\bar{p} = H[t]$ (see Figure 8 on the right). For the discretization phase, the boundary Γ has been approximated introducing a decomposition in 24 straight elements, equipped with linear shape functions. The time interval of analysis $[0, 12\,\pi]$ has been discretized with $\Delta t = \pi/10$. In Figure 10, on the left, the time history of the approximate solution $u(A,t)$ in the point A of the mesh, obtained with the energetic approach, is presented for this interior problem. For the sake of completeness, the approximate solution $u(A,t)$ of the exterior wave propagation problem, defined in $\Omega' = \mathbb{R}^2 \setminus \Omega$ with the same Neumann boundary conditions, obtained with the same discretization parameters, is shown on the right. This latter is in perfect agreement with that one reported in [**1**].

Acknowledgments. Work done within a research project financed by the Italian Ministry of University and of Research (MIUR) prot.2007JL35WY_002.

References

[1] A. I. Abreu, J. A. M. Carrer and W. J. Mansur, *Scalar wave propagation in 2D: a BEM formulation based on the operational quadrature method*, Eng. Anal. Bound. Elem. **27** (2003), 101-105.

[2] S. AHMAD and G. D. MANOLIS, *Dynamic analisys of 3-D structures by a transformed boundary element method*, Comput. Mech. **2** (1987), 185-196.

[3] A. AIMI, M. DILIGENTI and G. MONEGATO, *New numerical integration schemes for applications of Galerkin BEM to 2-D problems*, Internat. J. Numer. Methods Engrg. **40** (1997), 1977-1999.

[4] A. AIMI and M. DILIGENTI, *A new space-time energetic formulation for wave propagation analysis in layered media by BEMs*, Internat. J. Numer. Methods Engrg. **75** (2008), 1102-1132.

[5] A. AIMI, M. DILIGENTI, C. GUARDASONI, I. MAZZIERI and S. PANIZZI, *An energy approach to space-time Galerkin BEM for wave propagation problems*, Internat. J. Numer. Methods Engrg. **80** (2009), 1196-1240.

[6] A. AIMI, M. DILIGENTI and C. GUARDASONI, *Numerical integration schemes for the discretization of BIEs related to wave propagation problems*, in "Prooceedings of the 2009 International Conference CMMSE", J. Vigo-Aguiar, ed., Vol. I (2009), 45-56.

[7] A. AIMI, M. DILIGENTI and S. PANIZZI, *Energetic Galerkin BEM for wave propagation Neumann exterior problems*, CMES Comput. Model. Eng. Sci. **58** (2010), no. 2, 185-219.

[8] H. ANTES, *A boundary element procedure for transient wave propagations in two-dimensional isotropic elastic media*, Finite Elem. Anal. Des. **1** (1985), 313-322.

[9] A. BAMBERGER and T. HA DUONG, *Formulation variationnelle espace-temps pour le calcul par potentiel retardé de la diffraction d'une onde acoustique. I*, Math. Methods Appl. Sci. 8 (1986), 405-435.

[10] A. BAMBERGER and T. HA DUONG, *Formulation variationnelle pour le calcul de la diffraction d'une onde acoustique par une surface rigide*, Math. Methods Appl. Sci. 8 (1986), 598-608.

[11] M. COSTABEL, *Developments in boundary element methods for time-dependent problems*, in "Problems and methods in mathematical physics", Teubner-Texte Math., **134**, Teubner, Stuttgart 1994, 17-32.

[12] M. COSTABEL, *Time-dependent problems with the boundary integral equation method*, in "Encyclopedia of computational mechanics", Vol. 1, E. Stein, R. de Borst, T. J. R. Hughes, eds. , John Wiley & Sons, Chichester 2004, Chapter 25.

[13] T. A. CRUSE and F. J. RIZZO, *A direct formulation and numerical solution of the general transient elastodynamic problem. I*, J. Math. Anal. Appl. **22** (1968), 244-259.

[14] D. ELLIOT and D. F. PAGET, *Product-integration rules and their convergence*, BIT **16** (1976), 32-40.

[15] A. FRANGI, *Elastodynamics by BEM: a new direct formulation*, Internat. J. Numer. Methods Engrg. **45** (1999), 721-740.

[16] A. FRANGI and G. NOVATI, *On the numerical stability of time-domain elastodynamic analyses by BEM*, Comput. Methods Appl. Mech. Engrg. **173** (1999), 403-417.

[17] R. GALLEGO and J. DOMÍNGUEZ, *Hypersingular BEM for transient elastodynamics*, Internat. J. Numer. Methods Engrg. **39** (1996), 1681-1705.

[18] L. GAUL and M. SCHANZ, *A comparative study of three boundary element approaches to calculate the transient response of viscoelastic solids with unbounded domains*, Comput. Methods Appl. Mech. Engrg. **179** (1999), no. 1-2, 111-123.

[19] J. HADAMARD, *Lectures on Cauchy's problem in linear partial differential equations*, Yale Univ. Press, New Haven 1923.

[20] T. HA DUONG, *On retarded potential boundary integral equations and their discretization*, in "Topics in computational wave propagation", Lect. Notes Comput. Sci. Eng., 31, Springer, Berlin 2003, 301-336.

[21] T. HA DUONG, B. LUDWIG and I. TERRASSE, *A Galerkin BEM for transient acoustic scattering by an absorbing obstacle*, Internat. J. Numer. Methods Engrg. **57** (2003), 1845-1882.

[22] G. KRISHNASAMY, L. W. SCHMERR, T. J. RUDOLPHI and F. J. RIZZO, *Hypersingular boundary integral equations: some applications in acoustic and elastic wave scattering*, Trans. ASME J. Appl. Mech. **57** (1990), 404-414.

[23] C. LUBICH, *Convolution quadrature and discretized operational calculus. I*, Numer. Math. **52** (1988), 129-145.

[24] C. LUBICH, *Convolution quadrature and discretized operational calculus. II*, Numer. Math. **52** (1988), 413-425.

[25] C. LUBICH, *On the multistep time discretization of linear initial-boundary value problems and their boundary integral equations*, Numer. Math. **67** (1994), 365-389.

[26] G. MAIER, M. DILIGENTI and A. CARINI, *A variational approach to boundary element elastodynamic analysis and extension to multidomain problems*, Comput. Methods Appl. Mech. Engrg. **92** (1991), 193-213.

[27] W. J. MANSUR and C. A. BREBBIA, *Further developments on the solution of the transient scalar wave equation*, in "Topics in boundary element research", Vol. 2, C. A. Brebbia, ed., Springer, Berlin 1985, 87-123.

[28] G. D. MANOLIS and D. E. BESKOS, *Dynamic stress concentration studies by boundary integrals and Laplace transform*, Internat. J. Numer. Methods Engrg. **17** (1981), 573-599.

[29] G. MONEGATO, *Quadrature formulas for functions with poles near the interval of integration*, Math. Comp. **47** (1986), 301-312.

[30] G. MONEGATO, *The numerical evaluation of 2-D Cauchy principal value integral arising in boundary integral equation methods*, Math. Comp. **62** (1994), no. 206, 765-777.

[31] G. MONEGATO and L. SCUDERI, *Numerical integration of functions with boundary singularities*, J. Comput. Appl. Math. **112** (1999), 201-214.

[32] G. MONEGATO, *Product integration for one-dimensional integral equations of Fredholm type*, Atti Sem. Mat. Fis. Univ. Modena **40** (1992), no. 2, 653-666.

[33] G. MONEGATO, *Definitions, properties and applications of finite-part integrals*, J. Comput. Appl. Math. **229** (2009), 425-439.

[34] S. SIRTORI, *General stress analysis by means of integral equations and boundary elements*, Meccanica **14** (1979), 210-218.

[35] V. SLÁDEK and J. SLÁDEK, *Transient elastodynamic three-dimensional problems in cracked bodies*, Appl. Math. Modelling 8 (1984), 2-10.

[**36**] G. Szegö, *Orthogonal Polynomials*, Colloquium Publications, Vol. XXIII, American Mathematical Society, Providence, R.I. 1975.

[**37**] S. Wolfram, *The Mathematica*, 4th ed., Wolfram Media, Champaign, IL; Cambridge University Press, Cambridge 1999.

[**38**] Ch. Zhang, *A 2D hypersingular time-domain traction BEM for transient elastodynamic crack analysis*, Wave motion **35** (2002), 17-40.

Alessandra Aimi
University of Parma
Department of Mathematics
Parco Area delle Scienze 53/A
43124 Parma, Italy
e-mail: alessandra.aimi@unipr.it

Mauro Diligenti
University of Parma
Department of Mathematics
Parco Area delle Scienze 53/A
43124 Parma, Italy
e-mail: mauro.diligenti@unipr.it

Chiara Guardasoni
University of Parma
Department of Mathematics
Parco Area delle Scienze 53/A
43124 Parma, Italy
e-mail: chiara.guardasoni@unipr.it